NUMERICAL SOLUTION OF MICROPOLAR FLUID DUE TO MOVING SURFACE

STUDENT NAME: TUFAIL ABBAS
ENROLLMENT NO: 01-248202-003
SUPERVISOR BY DR. RIZWAN UL HAQ

A thesis submitted in fulfilment of the requirements for the awardof degree of Masters of Science (Mathematics)

Department of Computer Science

BAHRIA UNIVERSITY ISLAMABAD

Session (2020-2022)

Approval of Examination

Scholar Name: TUFAIL ABBAS

Registration Number: 71095

Enrollment: 01-248202-003

Program of Study: MS (Mathematics)

Thesis Title: Numerical Solution of Micropolar Fluid due to moving surface.

It is to certify that the above scholar's thesis has been completed to my satisfaction and, to my belief, its standard is appropriate for submission for examination. I have also conducted plagiarism test of this thesis using HEC prescribed software and found similarity index 17 % that is within the permissible limit set by the HEC for the MS/M.Phil degree thesis. I have also found the thesis in a format recognized by the BU for the MS/M.Phil thesis.

Supervisor Name: Dr. Rizwan ul Haq

Supervisor Signature:

Date:

Author's Declaration

I, TUFAIL ABBAS here by state that my MS/MPhill thesis titled "Numerical Solution of Micropolar Fluid due to moving surface" is my own work and has not been submitted previously by me for taking any degree from this Bahria University or anywhere else in the country/world. At any time if my statement is found to be incorrect even after my Graduate the university has the right to withdraw/cancel my MS/MPhill degree.

Name of Scholar: TUFAIL ABBAS

Date: 15/9/2022

Plagiarism Undertaking

I, solemnly declare that research work presented in the thesis titled "Numerical Solution of Micropolar Fluid due to moving surface" is solely my research work with no significant contribution from any other person. Small contribution/help wherever taken has been duly acknowledge and that complete thesis has been written by me.

I understand the zero tolerance policy of the HEC and Bahria University towards plagiarism. Therefore, I as an Author of the above title thesis declare that no portion of my thesis has been plagiarized and any material used as reference is properly referred/cited.

I undertake that if I am found guilty of any formal plagiarism in the above titled thesis even after award of MS/MPhill degree, the university reserves the right to withdraw/revoke my MS/MPhill degree and that HEC and the University has the right to publish my name on the HEC/University website on which names of students are placed who submitted plagiarized thesis.

Name of the Scholar: Tufail Abbas

Date:15/09/2022

Dedication

I dedicate my thesis work to my father (late) and mother. A special feeling of gratitude to my brothers and sisters. I will always appreciate all they have done for me. Dedicated to my wife, son and daughters whose words of encouragement and push for determination ring in my ears.

Acknowledgements

I am thankful to **ALLAH** (S.W.T) and his messenger, **Prophet Muhammad** (S.A.W). I also express my gratitude to Allah for giving me an opportunity to do this thesis successfully. It is because of the blessing of Allah who has enabled me to learn and to achieve desire towards my destination.

A special thanks to **Dr. Rizwan-ul-Haq**, my supervisor for his countless hours of reflecting, reading, encouraging, and most of all patience throughout the entire process. His valuable expertise, comments, suggestions, and instructions are most welcome that greatly improved the clarity of this thesis. I am so grateful to work under the supervision of such a great, kind, and diligent person.

My gratitude is to my honorable professors who took me to the apex of my academia with their guidance. In particular, **Prof. Dr. Muhammad Ramzan** and **Dr. Jaffar Hasnain** who have always been supportive in all of my course work and kept encouraging me throughout the session in Bahria University, Islamabad Campus. They are the true teachers who have started Mathematics program in BUIC, a real place of learning.

My intense recognition is to my mother, brothers, sister and wife who are always real pillars for my encouragement and showered their everlasting love, care, and support throughout my life. Humble prayers, continuing support and encouragement of my family are as always highly appreciated.

As usual, so many friends and my classmates have helped me throughout my MS that I cannot list them all. In particular, my college colleagues Ali Raza and Syed Asad Ali Shah were specially remained enormously helpful throughout the period of my MS studies.

Consequently, my all plea is to **Allah**, the Almighty, the beneficent Whose blessings are always showered upon me via strengthening my wisdom and bestowed me with the knowledge of what **Allah** wants.

Abstract

The major goal of writing this thesis to enunciate the notion of numerical solution of micropolar fluids due to moving surface. We have established the thesis in the following manners. In the first chapter, comprehensive study based upon literature is discussed for micropolar fluid. Second chapter consists of basic definitions of fluids and fundamental laws. Third chapter is a review chapter of micropolar fluid with magneto hydrodynamics along with viscous dissipation on a stretched sheet. By applying the built-in bvp4c approach with the similarity transformation, we have investigated a methodology of partial differential equations. Boundary layer approach is utilized to obtain the simplified form partial differential equations. Later on, by employing appropriate methods, boundary layer strategy and the similarity transformations, governing systems of PDE's has been converted to a various cumulative ODE's and then solved numerically. Graphically, the associated parameters including Prandtl number, magnetic parameter, material parameter, Eckert number, thermophoresis parameter, Brownian motion number and Schmidt number are variated for velocity and temperature profiles. In chapter four, micropolar fluid flow with zero mass flux of nanoparticles in a porous medium. The same strategy is used to solve the model as discussed for chapter 3. In the fifth chapter, the conclusion of the entire study is presented.

Table of Contents

List of figures

List of Symbols

b	constant
B_0	magnetic field
C	concentration of the fluid within boundary layer
D_B	Brownian diffusion coefficient
D_T	thermophoresis diffusion coefficient
N_b	Brownian motion parameter
N_t	thermophoresis parameter
$\tilde{N}u_x$	Nusselt number
Pr	Prandtl number
$\tilde{q}_w$	rate of heat transfer
$\tilde{R}e_w$	local Reynolds number
Sc	Schmidt number
C_f	skin friction coefficient
C_p	specific heat at aconstant pressure
C_W	concentration at the wall surface
C_∞	concentration of the fluid out side the boundary layer
E_c	Eckert number
$\tilde{h}_x$	heat flux transfer coefficient
k	vortex viscosity
k_f	thermal conductivity

K	material parameter
$\widetilde{N}$	dimensionless component of microroatation
$\tilde{T}$	temperature of boundary layer
$\tilde{T}_w$	temperature of surface
$\tilde{T}_\infty$	temperature outside the boundary

CHAPTER 1

FUNDAMENTAL CONCEPTS AND DEFINITIONS

Some of the fundamental definitions and few laws associated with the flow of fluid have been discussed in this chapter, briefly.

1.1 Fluid

A material that deforms continually under forced shear stress or external pressure is fluid. Fluids are a substance form of liquids, gases, and plasma.

1.2 Fluid mechanics

The analysis of both static and mobile fluids is called fluid mechanics. Fluid mechanics examine fluid behavior, both static and in motion. The contact of liquids with boundaries is also discussed. Fluid dynamics, kinematics and statics are subdivision of fluid mechanics into three categories. The movement of fluid particles is studied in fluid dynamics. Fluid Kinematics deals with study of movement of particles of the fluids with zero external forces and at rest the analysis of fluid's particles is called fluid statics.

1.3 Physical Properties of Fluid

1.3.1 Density of fluid

Mass (m) per unit volume (V) of particles of fluids is called the density (ρ) of fluid. Mathematically it can be expressed as:

$$\rho = \frac{m}{v}$$

$[ML^{-3}]$ is the dimension of density.

1.3.2 Dynamic viscosity

For any application when we study fluid flow, viscosity is a basic material property. The internal fluid resistance estimation is dynamic viscosity also called absolute viscosity and is represented by Greek letter μ. It can be mathematically written as:

$$\mu = \frac{\text{shear stress}}{\text{deformation rate}}$$

$[L^2T^{-1}]$ is dimension of dynamic viscosity.

1.3.3 Kinematic viscosity

The kinematic viscosity of fluids can be defined as the ratio between the absolute viscosity and density of fluid. Mathematically, it is represented by ν and written as

$$\nu = \frac{\text{absolute viscosity}}{\text{density}} = \frac{\mu}{\rho}$$

$\frac{m^2}{s}$ is the SI unit of ν.

1.4 Classification of fluid

1.4.1 Inviscid fluid

The fluid whose viscosity is zero is termed as inviscid fluid and also known as ideal fluid.

1.4.2 Viscous fluid

In viscous fluid viscosity does not vanish and viscous fluid is also termed as real fluid. Real fluid is of two types i.e.,

i. Newtonian
ii. Non - Newtonian fluid

i. Newtonian fluid

A viscous fluid known as a Newtonian fluid has a linear relationship between the shear stress and the rate of deformation. The Newton's viscosity law holds for such type of fluids. i.e.

$$\tau_{yx} \propto \frac{du}{dy} \Longrightarrow \tau_{yx} = \mu \frac{dy}{dx}$$

In the above expression, the proportionality constant is μ i.e. the fluid's dynamic viscosity.

ii. Non - Newtonian fluid

Non-Newtonian fluid is a kind of viscous fluid in which the relation between shear stress τ_{yx} and the rate of deformation $\left(\frac{du}{dy}\right)^n$ is inverse. ketchup, paint, blood, drilling muds, biological fluids etc. The power law model holds for such type of fluids i.e.

$$\tau_{yx} \propto \left(\frac{du}{dy}\right)^n \Rightarrow \tau_{yx} = k\left(\frac{du}{dy}\right)^n \quad , \qquad\qquad n \neq 1$$

where flow behavior index is n and consistency index is κ.

1.4.3 Compressible fluid

Compressible fluid is the fluid whose density varies continuously during its flow. At its each point the density of such fluids is different. All the gases fall in the category of compressible fluids.

1.4.4 Incompressible fluid

Incompressible fluid is the fluid whose density remains same during its flow. The value of density of such fluid is roughly same as its each point. Most famous example of incompressible fluids is water.

1.5 Two-Dimensional flow

The measurements are basically space coordinates and fluid motion in the majority of the scenarios is known to be tri dimensional, but two-dimensional is considered in order to make sure that the fluid flow is in plain coordinates and can be conveniently handled.

1.6 Boundary layer

A thin fluid layer behaves such that its inner surface permanently attached to the body's border. The flow's velocity is zero at the boundary. For a small layer velocity will change w.r.t distance from the surface. Velocity gradient exists for a small layer above the surface and this small layer is boundary layer. So, there will be some shear stress τ.

$$\tau = \mu \frac{du}{dy}$$

1.7 Nanofluid Flow

Nano-meter sized particles are known as nanoparticles. These types of fluids containing nanometer size particles is known as nanofluid. Fluid's nanoparticles are used to increase the fluid's thermal conductivity.

1.8 Brownian Motion

The haphazard and random motion experienced by the fluid's particles due to their collision with one another is known as the Brownian motion. e.g. Diffusion of pollutants in the air.

1.9 Thermophoresis

When mobile particles are mixed together, a process known as thermophoresis occurs in which the various particle types react differently to the force of a temperature gradient. In simple terms, the particle will be drawn to a cold surface and repelled away from a heated surface.

1.10 The Buoyant force

The buoyant force, sometimes referred to as up thrust, is the upward force generated on an element fully or partly submerged in the fluid is the buoyant force also known as up thrust. Because of the buoyant force, a body that is partly or fully immersed in a fluid feels lighter

1.11 Some useful non-dimensional numbers

1.11.1 Prandtl number

It is change in kinematic viscosity ν with respect to thermal diffusivity α. It is non-dimensional number. Mathematically,

$$Pr = \frac{\nu}{\alpha}$$

1.11.2 Reynolds number

Reynolds number is a non-dimensional ratio of the fluid's inertial and viscous forces. Mathematically,

$$\tilde{R}e = \frac{\alpha x^2}{\nu}$$

1.11.3 Nusselt number

The non-dimensional ratio of the fluid's convective and conductive heat transfer is called Nusselt number. This may be measured using flux, which also gives the speed at which heat is transferred from a surface to a fluid.

1.11.4 Sherwood number

Dimensionless ratio in the convective mass transfer and the mass transport diffusion's rate is Sherwood number.

1.11.5 Eckert number

The fractional relation of kinetic energy and enthalpy is characterized termed Eckert number. Generally, it can be expressed as;

$$Ec = \frac{\text{advective mass transfer}}{\text{viscous dissipation}}$$

1.12 Conservation laws

To deal with conserved quantity we use laws of conservation. Laws of conservation specified below are used for flow specification in the sub sequential analysis.

- Momentum conservation law
- Energy conservation law
- Concentration law of conservation

1.12.1 Conservation of Mass

The conservation of mass can be used to derive the continuity equation and mathematically, it is expressed by

$$\frac{\partial \rho}{\partial t} + \tilde{\nabla} . \left(\rho \tilde{V}\right) = 0,$$

where t is the time. In case of an incompressible fluid, the continuity equation is expressed by

$$\tilde{\nabla}.\tilde{V} = 0,$$

1.12.2 Law of Conservation of Energy with Brownian and Thermophoresis effects

Energy equation for fluids is

$$\rho C_p \left(\frac{\partial}{\partial t} + \tilde{V}\tilde{\nabla}\right)\tilde{T} = \kappa\tilde{\nabla}^2\tilde{T} + \tau L + \rho C_p \left[D_B\tilde{\nabla}C.\tilde{\nabla}\tilde{T} + \frac{D_B}{D_T}\,\tilde{\nabla}\tilde{T}\right],$$

where C_p denotes the basic fluid's specific heat, ρ is density for fluid's particle and rate of strain tensor represented by L, the fluid's temperature denoted as $\tilde{T}$, the coefficient of Brownian motion denoted by D_B and temperature diffusion coefficient by D_T.

CHAPTER 2

INTRODUCTION

Research in exceptional areas has been offered by fluid mechanics. The continuing advancement of fluid mechanics theory and applications has been facilitated by researchers. The most deep-rooted Model of Navier-Stokes for classical fluids presents that the motions of Newtonian fluids that seem to be incompressible. Nevertheless, Navier-Stokes representation is insufficient to explain the liquids like polar fluids, fluids with microstructural components. These fluids are fascinating on their own and essential from a practical one. Most of these consisting of the Polymeric suspensions, blood of animals, crystals of liquid characterize these fluids that are complex. Their constituent particles could enlarge and contract, their shapes might vary, and they have the ability to rotate independently.

Several explanations have been proposed, Despite the fact that basic deformable directed fluids, simple micro fluid theories, and dipolar fluids all resemble the type of fluids containing microstructure, they are not all universal. Eringen [1, 2] was the first to develop the theory of microfluids, which thoroughly investigates the Navier-Stokes model. The microscopic movement and local structure for the fundamental elements of fluid are associated to microscopic effects that have been seen in microfluids. Spin inertia has an impact on such fluids, which can withstand tension and bodily movements.

Eringen [3] then advanced the notion of micropolar fluids. This theory contains established fluid medium that is under stress along with micro rotational effects, micro rotational inertia, and couple stresses. He examined flow problems of one-dimension for micropolar fluids. He worked at one-dimensional micropolar fluid flow problems. Furthermore particular, he examined the uniform flow of micropolar fluids in different channels like ducts, tubes, circular and spherical. Specifically, and presented graphical representations for coupled stress, shear stress differences, velocity, and micro-rotation profiles.

Physically, this category of bar-like elements in the same approach with the fluids that are isotropic fluids, e.g. crystals of liquids, that together with molecules resembling dumbbell, blood of animals, fluids containing polymers and those fluids which have particular additives. This theory has been predicted to also offer a mathematical explanation for non-Newtonian behaviour seen in some synthetic liquids, such bloods and polymers.

Fundamental flow problems have been studied using Micropolar Fluid concepts framework. The research conducted in the field of micropolar fluid flow problems as well as its possible applications first described by Ariman et al. [4]. The flow of micropolar fluid past a permeable stretching sheet in presence of joule heating, thermal radiation, partial slip and magneto hydrodynamic (MHD) with convective boundary conditions have discussed by Ramzan, M et al. [5]. Turk et al. [6, 7], Hogen et al. [8,] have all applied the approach to blood flow. The steady two-dimensional stagnation point flow of an incompressible micropolar fluid over a stretching sheet when the sheet is stretched in its own plane with a velocity proportional to the distance from the stagnation point, has been studied by Nazar et al. [9]. Tozeren et al. [10] used the concept of micropolar fluids for suspensions. In contrast, Allen et al. [11] proposed the idea of a lubrication of the micropolar fluids. Making use of a finite difference method, Chapman and Bauer [12] were successful in finding a group of accurate solutions to the Navier-Stokes equations. For micropolar instance, this issue was looked into Agarwal [13], Takhar, and Soundalgekar [13,14] discussed the flow and heat transport of both micropolar fluid over a porous medium. Haq, R.U et al. [15] investigated the two-dimensional boundary-layer flow of natural convective micropolar nanofluid along a vertically stretching sheet. Moreover, considered the simultaneous effects of radiation and convective boundary surface. Influences of nanoparticles also analyzed for both assisting and opposing flow. A class of accurate solutions for the Magneto hydro-dynamics flow for micropolar fluids trapped between parallel, non-coaxial, insulated, and infinite spinning discs were studied by Kasiviswanathan and Gandhi [16]. Guram

[17] investigated the existence of in stationary flows of incompressible micropolar fluids and Smith [18] researched an accurate solution for the uniform Magneto hydrodynamics flow for a micropolar fluid is examined, together with the stationary flow for a micropolar fluids with powerful and fragile contact. Al-Sanea [19] examined mixed convection heat transfer with a constantly rotating heated vertical channel by investigating at suction or injection. Kumari and Nath [20] examined mixed convection boundary layer flow across a confined vertical cylinder along concentrated injection or suction and cooling or heating. Outside of a stretched empty cylinder, Wang [21] studied the flow in an acoustic fluid at rest that was viscous and incompressible. The effects of a shrinking sheet on Magneto hydrodynamic viscous flow were examined by Sajid and Hayat [22] using the homotopy analysis method. Sajid et al. [23] explored the magneto hydro-dynamic rotating flow of a viscous fluid over a contracting surface. In order to analyze Magneto hydro-dynamics flow for non-Newtonian fluid across stretched sheet, Liao [24] developed an analytical solution.

The two-dimensional boundary layer was examined by Kuiken [25] and Banks [26] Closed-form exact solutions of MHD viscous flow over a shrinking sheet. Ishak et al. [27] examined the effects for a constant hydrostatic pressure of flow and heat transfer outside a stretched porous cylinder and used the Keller-box technique for numerical solutions. Wang [28] investigated the stagnation flow in the direction of a contracting plate. According to his discussions the axisymmetric and two-dimensional examinations of this study are under consideration. A unique class of solutions with exact similarity and reverse flow examined in his study. Fang and Zhang [29] examined magneto hydro-dynamics flow along a shrinking surface and provided an accurate solution to the problem. Wang [30] proposed an accurate approximate solution for three-dimensional fluid dynamics in response for a stretched flat surface. Rahman et al. [31] conducted computational modeling to study the effect of fluid electric conductivity and non-uniform source of heat or sink to a two-dimensional, uniform, hydromagnetic, and convective flow for a micropolar fluid in contrast to fluid layer flow with a slanted solid surface with a homogeneous surface heat flux. Hayat et al. [32] studied the two-dimensional Magnetohydrodynamics unsteady flow for an incompressible micropolar fluid through a nonlinear stretching sheet. Ishak et al. [33] examined the continuous

Magnetohydrodynamics mixed convection stagnation flow for a vertical surface immersed in an incompressible micropolar fluid. Ishak et al. [34] investigated the stagnation flow for magnetohydrodynamics boundary layer flow in the presence of a changing magnetic field using a spike with a constant flux of surface heat covered in an incompressible micropolar fluid. The constant convective heat transfer boundary layer movement for a vertical surface immersed in an incompressible micropolar fluid is taken into consideration by Ishak et al [35] in the analysis. Tarek [36] investigates flow through the boundaries of a micro-polar fluid caused by continuously extended surface in the case of decreasing coupled variables. The constant convective heat transfer boundary layer movement across a vertical plane covered in a viscous fluid micropolar fluid described briefly a work by Ishak et al. [37]. Kumaran et al. [38] accurately solve for mixed convection flow for a liquid along an electrical conductivity through a nonlinearly extended and linear transparent surface. Nazar et al. [39] have investigated the movement of an incompressible micropolar fluid with the presence at a stable, two-dimensional stagnation flow when the sheet is extended inside the field with a speed proportionate the distance from the stagnation point. Hayat et al. [40] examined peristaltic flow for a micropolar fluid in a channel.

Examining numerical solution of Micropolar fluids due to moving surfaces is the objective of this study. For this the energy equation, momentum equation, angular momentum equation and concentration equations are employed using boundary layer approach. The PDEs have been transformed into ODEs using the suitable associated transformations. To attain the objective of numerical solution, the associated ODEs are solved numerically.

CHAPTER 3

MICROPOLAR NANOFLUID FLOW WITH MHD AND VISCOUS DISSIPATION EFFECTS TOWARDS A STRETCHING SHEET

The intention of writing this chapter is to investigate Numerical solution of Micropolar Nano-fluid flow with Magnetohydrodynamics and viscous dissipation effects towards a stretching sheet. The equations for energy, momentum, angular momentum and concentration are defined mathematically and then extracted. The boundary conditions are mentioned as well. In order to arrive at closed form solution of the equations of momentum, energy, angular momentum and concentration, we converted the governing nonlinear PDEs into dimensionless nonlinear ODEs. In order to numerically calculate the solution of dimensionless ODEs with boundary conditions, utilizing the built-in bvp4c approach after conversion of the given PDEs to the first order ODEs.

3.1 Mathematical Formulation of the problem

Consider a unidirectional, incompressible flow for micropolar fluid, nanofluids through a moving surface which is steady and two dimensional. A coordinate system used is a two-dimensional Cartesian system. Consider x-axis parallel to the surface, whereas y-axis is perpendicular to it. The strength of magnetic field B_0 is applied vertically of electrically conducting fluid. Governing equations Continuity, energy equation, momentum equation, angular momentum equation and concentration equation for this problem may be formulated using the usual boundary layer approach as follows:

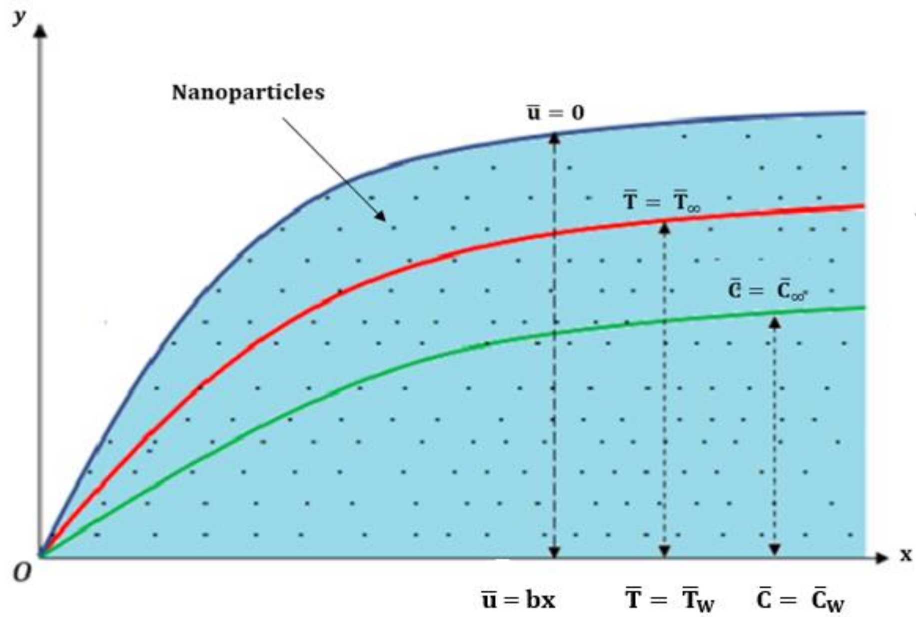

Figure 1. Geometry of model

$$\frac{\tilde{\partial}\rho}{\partial t} + \tilde{\nabla} . \left(\rho\tilde{V}\right) = 0, \tag{3.1}$$

$$(\lambda + 2\mu + \kappa)\tilde{\nabla}\left(\tilde{\nabla}.\tilde{V}\right) - (\mu + \kappa)\,\tilde{\nabla} \times \left(\tilde{\nabla} \times \tilde{V}\right) + \kappa\left(\tilde{\nabla} \times \tilde{N}\right) - \tilde{\nabla}\tilde{P} + \rho f^{*}$$

$$= \rho\left(\frac{\partial\tilde{V}}{\partial t} + \tilde{V} . \left(\tilde{\nabla}\tilde{V}\right)\right), \tag{3.2}$$

$$(\alpha + \beta + \gamma)\,\tilde{\nabla}\left(\tilde{\nabla} . \tilde{N}\right) - \gamma\left(\tilde{\nabla} \times \tilde{\nabla} \times \tilde{N}\right) + \kappa\left(\tilde{\nabla} \times \tilde{V}\right) - 2\kappa\tilde{N} + \rho\, l^{*}$$

$$= \rho j\left(\frac{\partial\tilde{N}}{\partial t} + \tilde{V} . \tilde{\nabla}\tilde{N}\right), \tag{3.3}$$

$$\rho C_p\left(\frac{\partial\tilde{T}}{\partial t} + \left(\tilde{V}.\tilde{\nabla}\right)\tilde{T}\right) = k\tilde{\nabla}^2\tilde{T}, \tag{3.4}$$

where ρ is density of fluid, $\tilde{V}$ is the velocity vector, microrotation is $\tilde{N}$, $\tilde{P}$ is pressure, body force and body couple per unit mass are f^{*} and l^{*} respectively, the microinertia is j,material constants are $\alpha, \beta\ , \gamma\ , \mu\ , \lambda$ while fluid's temperature ($\tilde{T}$), specific heat of fluid (C_P) and conductivity of heat (k) respectively. Body couples are also ignored, and steady, laminar, incompressible fluid flow problems are assumed to exist. The equations (3.1) to (3.4) become based on the above-mentioned assumptions.

$$\tilde{\nabla}.\tilde{V} = 0, \tag{3.5}$$

$$\kappa\left(\tilde{\nabla} \times \tilde{N}\right) - (\mu + \kappa)\,\tilde{\nabla} \times \left(\tilde{\nabla} \times \tilde{V}\right) - \tilde{\nabla}P + \rho f = \rho\left(\tilde{V}.\tilde{\nabla}\right)\tilde{V}, \tag{3.6}$$

$$(\alpha + \beta + \gamma)\,\tilde{\nabla}\left(\tilde{\nabla}.\tilde{N}\right) - \gamma\left(\tilde{\nabla} \times \tilde{\nabla} \times \tilde{N}\right) + \kappa\left(\tilde{\nabla} \times \tilde{V}\right) - 2\kappa\tilde{N} = \rho j\left(\tilde{V}.\tilde{\nabla}\tilde{N}\right), \tag{3.7}$$

$$\rho\, C_p\left(\tilde{V}.\tilde{\nabla}\right)\tilde{T} = k\tilde{\nabla}^2\tilde{T}, \tag{3.8}$$

The velocity components $\bar{V} = \bar{V}(u, v, w)$ and microrotation $\bar{N} = \bar{N}\,(N_1, N_2, N_3)$ may be used to write the above set of equations (3.5) to (3.8) can be written in Cartesian coordinates system.

The components of associated partial differential equations are:

$$\frac{\partial\tilde{u}}{\partial x} + \frac{\partial\tilde{v}}{\partial y} + \frac{\partial\tilde{w}}{\partial z} = 0, \tag{3.9}$$

$$(\mu + \kappa)\left(\frac{\partial^2\tilde{u}}{\partial x^2} + \frac{\partial^2\tilde{u}}{\partial y^2} + \frac{\partial^2\tilde{u}}{\partial z^2}\right) + \kappa\left(\frac{\partial\tilde{N}_3}{\partial y} - \frac{\partial\tilde{N}_2}{\partial z}\right) - \frac{\partial P}{\partial x} + \rho f_x$$

$$= \rho\left(\tilde{u}\,\frac{\partial\tilde{u}}{\partial x} + \tilde{v}\,\frac{\partial\tilde{u}}{\partial y} + \tilde{w}\,\frac{\partial\tilde{u}}{\partial z}\right), \tag{3.10}$$

$$(\mu + \kappa)\left(\frac{\partial^2\tilde{v}}{\partial x^2} + \frac{\partial^2\tilde{v}}{\partial y^2} + \frac{\partial^2\tilde{v}}{\partial z^2}\right) + \kappa\left(\frac{\partial\tilde{N}_1}{\partial z} - \frac{\partial\tilde{N}_3}{\partial x}\right) - \frac{\partial P}{\partial y} + \rho f_y$$

$$= \rho\left(\tilde{u}\,\frac{\partial\tilde{v}}{\partial x} + \tilde{v}\,\frac{\partial\tilde{v}}{\partial y} + \tilde{w}\frac{\partial\tilde{v}}{\partial z}\right), \tag{3.11}$$

$$(\mu + \kappa)\left(\frac{\partial^2\tilde{w}}{\partial x^2} + \frac{\partial^2\tilde{w}}{\partial y^2} + \frac{\partial^2\tilde{w}}{\partial z^2}\right) + \kappa\left(\frac{\partial\tilde{N}_2}{\partial x} - \frac{\partial\tilde{N}_1}{\partial y}\right) - \frac{\partial P}{\partial z} + \rho f_z$$

$$= \rho\left(\tilde{u}\,\frac{\partial\tilde{w}}{\partial x} + \tilde{v}\,\frac{\partial\tilde{w}}{\partial y} + \tilde{w}\,\frac{\partial\tilde{w}}{\partial z}\right), \tag{3.12}$$

$$(\alpha+\beta+\gamma)\left(\frac{\partial}{\partial x}\left(\frac{\partial \widetilde{N}_1}{\partial x}+\frac{\partial \widetilde{N}_2}{\partial y}+\frac{\partial \widetilde{N}_3}{\partial z}\right)\right)+\kappa\left(\frac{\partial \widetilde{w}}{\partial y}-\frac{\partial \widetilde{v}}{\partial z}\right)-2\kappa \widetilde{N}_1$$
$$-\gamma\left(\frac{\partial}{\partial x}\left(\frac{\partial \widetilde{N}_1}{\partial x}+\frac{\partial \widetilde{N}_2}{\partial y}+\frac{\partial \widetilde{N}_3}{\partial z}\right)-\left(\frac{\partial^2 \widetilde{N}_1}{\partial x^2}+\frac{\partial^2 \widetilde{N}_1}{\partial y^2}+\frac{\partial^2 \widetilde{N}_1}{\partial z^2}\right)\right)$$
$$=\rho j\left(\tilde{u}\,\frac{\partial \widetilde{N}_1}{\partial x}+\tilde{v}\,\frac{\partial \widetilde{N}_1}{\partial y}+\widetilde{w}\,\frac{\partial \widetilde{N}_1}{\partial z}\right), \qquad (3.13)$$

$$(\alpha+\beta+\gamma)\left(\frac{\partial}{\partial y}\left(\frac{\partial \widetilde{N}_1}{\partial x}+\frac{\partial \widetilde{N}_2}{\partial y}+\frac{\partial \widetilde{N}_3}{\partial z}\right)\right)+\kappa\left(\frac{\partial \tilde{u}}{\partial z}-\frac{\partial \widetilde{w}}{\partial x}\right)-2\kappa \widetilde{N}_2$$
$$-\gamma\left(\frac{\partial}{\partial y}\left(\frac{\partial \widetilde{N}_1}{\partial x}+\frac{\partial \widetilde{N}_2}{\partial y}+\frac{\partial \widetilde{N}_3}{\partial z}\right)-\left(\frac{\partial^2 \widetilde{N}_2}{\partial x^2}+\frac{\partial^2 \widetilde{N}_2}{\partial y^2}+\frac{\partial^2 \widetilde{N}_2}{\partial z^2}\right)\right)$$
$$=\rho j\left(\tilde{u}\,\frac{\partial \widetilde{N}_2}{\partial x}+\tilde{v}\,\frac{\partial \widetilde{N}_2}{\partial y}+\widetilde{w}\,\frac{\partial \widetilde{N}_2}{\partial z}\right), \qquad (3.14)$$

$$(\alpha+\beta+\gamma)\left(\frac{\partial}{\partial z}\left(\frac{\partial \widetilde{N}_1}{\partial x}+\frac{\partial \widetilde{N}_2}{\partial y}+\frac{\partial \widetilde{N}_3}{\partial z}\right)\right)+\kappa\left(\frac{\partial \tilde{v}}{\partial x}-\frac{\partial \tilde{u}}{\partial y}\right)-2\kappa \widetilde{N}_3$$
$$-\gamma\left(\frac{\partial}{\partial z}\left(\frac{\partial \widetilde{N}_1}{\partial x}+\frac{\partial \widetilde{N}_2}{\partial y}+\frac{\partial \widetilde{N}_3}{\partial z}\right)-\left(\frac{\partial^2 \widetilde{N}_3}{\partial x^2}+\frac{\partial^2 \widetilde{N}_3}{\partial y^2}+\frac{\partial^2 \widetilde{N}_3}{\partial z^2}\right)\right)$$
$$=\rho j\left(\tilde{u}\,\frac{\partial \widetilde{N}_3}{\partial x}+\tilde{v}\,\frac{\partial \widetilde{N}_3}{\partial y}+\widetilde{w}\,\frac{\partial \widetilde{N}_3}{\partial z}\right), \qquad (3.15)$$

$$\rho C_p\left(\tilde{u}\frac{\partial \tilde{T}}{\partial x}+\tilde{v}\frac{\partial \tilde{T}}{\partial y}+\widetilde{w}\frac{\partial \tilde{T}}{\partial z}\right)=k\left(\frac{\partial^2 \tilde{T}}{\partial x^2}+\frac{\partial^2 \tilde{T}}{\partial y^2}+\frac{\partial^2 \tilde{T}}{\partial z^2}\right), \qquad (3.16)$$

$$\tilde{u}\frac{\partial \tilde{C}}{\partial x}+\tilde{v}\frac{\partial \tilde{C}}{\partial y}=D_B\frac{\partial^2 \tilde{C}}{\partial y^2}+\frac{D_T}{T_\infty}\frac{\partial^2 \tilde{T}}{\partial y^2}\,, \qquad (3.17)$$

By selecting velocity field of the form:

$$\tilde{V}=[u(x,y),\ v(x,y),0], \qquad (3.18)$$

The following boundary layer approximations are employed to get the boundary layer equations.

$$\tilde{x} = \frac{x^*}{L}\ ,\ \tilde{y} = \frac{y^*}{\delta}\ ,\tilde{u} = \frac{u}{U}\ ,\tilde{v} = \frac{vL}{U\delta}\ ,\tilde{P} = \frac{p^*}{\rho U^2}\ ,t = \frac{t^* U}{L}\ ,\tilde{N} = \frac{N}{U}, \tag{3.19}$$

Now, using velocity field (3.18) and the boundary layer approximations (3.19) in equations (3.9) to (3.17). Continuity equation holds and by neglecting body forces nonlinear partial differential equations of momentum, the angular momentum yield (3.20) to (3.24) and so there is no change in pressure across the boundary layer. Also, it implies that $\tilde{\mathrm{P}}$ is just a function of x. The inviscid flow beyond the boundary layer alone determines the pressure forces acting on a body.

$$\frac{\partial \tilde{u}}{\partial x} + \frac{\partial \tilde{v}}{\partial y} = 0, \tag{3.20}$$

$$\rho\left(\tilde{u}\ \frac{\partial \tilde{u}}{\partial x} + \tilde{v}\ \frac{\partial \tilde{u}}{\partial y}\right) = (\mu + \kappa)\left(\frac{\partial^2 \tilde{u}}{\partial y^2}\right) + \kappa\ \left(\frac{\partial \tilde{N}}{\partial y}\right) - \sigma B_0^2\ \tilde{u}, \tag{3.21}$$

$$\rho j\left(\tilde{u}\ \frac{\partial \tilde{N}}{\partial x} + \tilde{v}\frac{\partial \tilde{N}}{\partial y}\right) = \gamma\frac{\partial^2 \tilde{N}}{\partial x^2} + \kappa\left(\frac{\partial \tilde{N}}{\partial y} + 2\tilde{N}\right), \tag{3.22}$$

$$\rho C_p\left(\tilde{u}\frac{\partial \tilde{T}}{\partial x} + \tilde{v}\ \frac{\partial \tilde{T}}{\partial y}\right) = k\left(\frac{\partial^2 \tilde{T}}{\partial y^2}\right) + (\mu + \kappa)\left(\frac{\partial \tilde{u}}{\partial y}\right)^2 + \sigma B_0^2\ \tilde{u}^2 + \frac{(\rho Cp)_p}{(\rho Cp)_f}\left[D_B\frac{\partial C}{\partial y}\frac{\partial \tilde{T}}{\partial y} + \frac{D_T}{D_B}\left(\frac{\partial \tilde{T}}{\partial y}\right)^2\right], \tag{3.23}$$

$$\tilde{u}\ \frac{\partial \tilde{C}}{\partial x} + \tilde{v}\frac{\partial \tilde{C}}{\partial y} = D_B\frac{\partial^2 \tilde{C}}{\partial x^2} + \frac{D_T}{T_\infty}\frac{\partial^2 \tilde{T}}{\partial y^2}, \tag{3.24}$$

The associated BCs of equation (3.20) to (3.24) are:

$$\tilde{u} = \tilde{v}_w = bx^*, \tilde{v} = 0,\ \ \tilde{N} = 0,\ \ \tilde{T} = \tilde{T}_w, \tilde{C} = \tilde{C}_w\ ,\quad at\ \ \tilde{y} = 0 \tag{3.25a}$$

$$\tilde{u} = 0, \tilde{N} = 0, \tilde{T} = \tilde{T}_\infty\ ,\ \tilde{C} = \tilde{C}_\infty\ ,\qquad as\ \ \tilde{y} \to \infty \tag{3.25b}$$

Converting the governed PDE's (3.20), (3.21), (3.22), (3.23) and (3.24) into dimensionless non-linear ODE's, the similarity variables mentioned below are utilized to convert the equation system:

$$\tilde{\eta} = \sqrt{b/\nu_f}\ \tilde{y}\ , \tilde{u} = b\tilde{x}\ f'(\eta), \tilde{v} = -\sqrt{b\nu_f}f(\eta),\ \tilde{N} = \sqrt{b^3/\nu_f}\,\tilde{x}g(\eta), \tag{3.26a}$$

$$\tilde{\theta}(\eta) = \frac{\tilde{T}-\tilde{T}_\infty}{\tilde{T}_w-\tilde{T}_\infty}, \; \tilde{T} = \tilde{T}_\infty + A\tilde{x}\theta(\eta), \; \tilde{\phi}(\eta) = \frac{\tilde{C}-\tilde{C}_\infty}{\tilde{C}_w-\tilde{C}_\infty}, \; \tilde{C} = \tilde{C}_\infty + B\tilde{x}\phi(\eta), \tag{3.26b}$$

The velocity components from the stream function $\psi(x, y)$ will be

$$\tilde{u} = \tilde{\psi}_y \;, \quad \tilde{v} = -\tilde{\psi}_x. \tag{3.26c}$$

Applying similarity transformations (3.26a) and (3.26b) it satisfies continuity equation and the equations (3.21), (3.22), (3.23) and (3.24) takes the following form;

$$(1+K)f''' + ff'' - f'^2 + Kg' - Mf' = 0, \tag{3.27}$$

$$(1+K/2)g'' + fg' - f'g - K(2g + f'') = 0, \tag{3.28}$$

$$\theta'' + Prf\theta' + (1+K)PrEcf''^2 + PrEcMf'^2 + PrNb\theta'\phi' + PrNt\theta'^2 = 0, \tag{3.29}$$

$$\phi'' + Scf\phi' - Scf'\phi + \frac{N_t}{N_b}\theta'' = 0, \tag{3.30}$$

Where,

$$K = \frac{\kappa}{\mu}, \quad Pr = \frac{c_p\mu}{k_\infty}, \quad M = \frac{\sigma B_0^2}{\rho b}, \quad Ec = \frac{\tilde{u}_w^2}{c_\rho\,(\tilde{T}_w-\tilde{T}_\infty)}$$

$$N_b = \frac{(\rho Cp)_p\, D_B\,(\tilde{C}_w-\tilde{C}_\infty)}{(\rho Cp)_f\;\nu_f}, \quad N_t = \frac{(\rho Cp)_p\, D_T\,(\tilde{T}_w-\tilde{T}_\infty)}{(\rho Cp)_f\;\nu_f\;\tilde{T}_\infty}$$

Boundary conditions take the following form:

$$f(\eta=0) = 0, \;\; f'(\eta=0) = \theta(\eta=0) = \phi(\eta=0) = 1 \tag{3.31a}$$

$$f'(\eta\to\infty) = g(\eta\to\infty) = \theta(\eta\to\infty) = \phi(\eta\to\infty) = 0 \tag{3.31b}$$

The flux at the surface is given by

$$\tilde{q}_w(x) = -k_f\left(\frac{\partial\tilde{T}}{\partial y}\right)_{y=0} = -k_f(\tilde{T}_w - \tilde{T}_\infty)\sqrt{\frac{b}{\nu_f}}\theta'(0), \tag{3.32}$$

By using eq (3.26a) and (3.26b), simplifying we get

$$\tilde{\tau}_w = (k+\mu)_f b\tilde{x}\sqrt{\frac{b}{\nu_f}}\, f''(0), \tag{3.33}$$

Make use of $\tilde{u}_w = b\tilde{x}$, the definition of skin friction coefficient C_f as a characteristic velocity is

$$c_f = \frac{\tilde{\tau}_w}{\rho_f \tilde{u}_w^2}, \tag{3.34}$$

Putting Eq. (3.26a) and (3.26 b) into Eq. (3.32) and (3.33), we get

$$C_f\sqrt{\tilde{R}e_w} = (1+\tilde{K})\,|f''(0)|, \tag{3.35}$$

Where local Reynolds number is.

$$Re_w = \frac{b\tilde{x}^2}{\nu_f},$$

Couple stress at the surface is expressed as:

$$\tilde{M}_w = \gamma\left(\tilde{T}_y\right)_{y=0} = \rho_f b\tilde{u}_w\left(1+\frac{K}{2}\right)|g'(0)|, \tag{3.36}$$

$$\tilde{h}_x = \frac{\tilde{q}_w(x)}{(\tilde{T}_w - \tilde{T}_\infty)}, \tag{3.37}$$

The local Nusselt number may be expressed as

$$\tilde{N}u_x = \frac{\tilde{x}\tilde{h}(x)}{k_f} = -\sqrt{\frac{b}{\nu_f}}\,\tilde{x}\theta'(0), \tag{3.38}$$

Or

$$\frac{\tilde{N}u_x}{\sqrt{Re_w}} = -\theta'(0), \tag{3.39}$$

Sherwood number can be written as

$$\tilde{S}h_x = -\sqrt{\frac{b}{\nu_f}}\tilde{x}\phi'(0), \tag{3.40}$$

Or $\frac{\tilde{S}h_x}{\sqrt{Re_w}} = -\phi'(0),$ (3.41)

3.2 Methodology

Numerically solving the non-linear differential equations along with BC's utilizing the built-in bvp4c approach after conversion of the given PDEs to the first order ODEs. We consider:

$f = y_1,$ $g = y_4$ $\theta = y_6,$ $\phi = y_8,$

$f' = y_2,$ $g' = y_5$ $\theta' = y_7,$ $\phi' = y_9,$

$f'' = y_3,$ $g'' = y_{11}$ $\theta'' = y_{12},$ $\phi'' = y_{13},$

$f''' = y_{10},$

$$Eq(3.27) \Rightarrow (1+K)y_{10} + y_1y_2 - y_2^2 + Ky_5 - My_2 = 0,$$

$$\Rightarrow y_{10} = \left(\frac{-y_1y_2 + y_2^2 - Ky_5 + My_2}{1+K}\right), \tag{3.42}$$

$$Eq(3.28) \Rightarrow \left(1+\frac{K}{2}\right)y_{11} + y_1y_5 - y_2y_4 - K(2y_4 + y_3) = 0,$$

$$\Rightarrow y_{11} = 2\left(\frac{-y_1y_5 + y_2y_4 + K(2y_4 + y_3)}{2+K}\right), \tag{3.43}$$

$$Eq(3.29) \Longrightarrow y_{12} + Pry_1y_7 + (1+K)PrEcy_3^2 + PrEcMy_2^2 + PrN_by_7y_9 = 0,$$

$$\Longrightarrow y_{12} = -Pry_1y_7 - (1+K)PrEcy_3^2 - PrEcMy_2^2 - PrN_by_7y_9, \tag{3.44}$$

$$Eq(3.30) \Longrightarrow y_{13} + Scy_1y_9 - Scy_2y_8 + \frac{N_t}{N_b}y_{12} = 0,$$

$$\Rightarrow y_{13} = -Scy_1y_9 + Scy_2y_8 - \frac{N_t}{N_b}y_{12}, \tag{3.45}$$

$$\Rightarrow \begin{bmatrix} f' \\ f'' \\ f'' \\ f''' \\ g' \\ g'' \\ \theta' \\ \theta'' \\ \phi \\ \phi'' \end{bmatrix} = \begin{bmatrix} y_2 \\ y_3 \\ y_{10} \\ y_5 \\ y_{11} \\ y_7 \\ y_{12} \\ y_9 \\ y_{13} \end{bmatrix} \begin{bmatrix} y_2 \\ y_3 \\ \left(\dfrac{-y_1y_2 + y_2^2 - Ky_5 + My_2}{1+K}\right) \\ y_5 \\ 2\left(\dfrac{-y_1y_5 + y_2y_4 + K(2y_4 + y_3)}{2+K}\right) \\ y_{11} \\ -Pry_1y_7 - (1+K)PrEcy_3^2 - PrEcMy_2^2 - PrN_by_7y_9 \\ y_9 \\ -Scy_1y_9 + Scy_2y_8 - \dfrac{N_t}{N_b}y_{12} \end{bmatrix}$$

3.3 Results and discussion

Examining the influence of dimensionless characteristics such as the Eckert number (*Ec*), material number (*K*), Prandtl number (*Pr*), magnetic number (*M*), thermophoresis parameter (*Nt*), Schmidt number (*Sc*) and Brownian motion number (*Nb*) is primary goal for this section. In this work, the concept of boundary layer is used to get a group of coupled momentum, energy, angular momentum and concentration equations in order to evaluate the flow, temperature, and concentration fields of the flow. A similarity transformation method is using for the transformation of the nonlinear coupled PDEs to a group of nonlinear coupled ODEs.

Figures (2) – (5) depicts the impacts of a magnetic number upon temperature distribution, concentration, angular velocity distribution, and velocity distribution. Figure (2) delineate impact of magnetic field parameter (*M*) upon velocity distributions. It is apparent, due to increased magnetic field, velocity has been declined. It is because of the fact that the drag force also referred as Lorentz force, appears when magnetic fields are used to the fluid. This force has the tendency to slow the fluid velocity in the boundary layer. Figure (3) illustrate impact of magnetic field parameter (M) upon angular velocity distributions. It is clear that, due to increased magnetic field, angular velocity has been reduced. Dimensionless temperature distributions are shown in Figure (4). The curves demonstrate that when the magnetic numbers are increasing, the dimensionless temperature profile also increases. Figure (5) illustrate impact of magnetic field parameter (M) upon concentration distributions. It is evident, due to increased magnetic field, concentration distributions have been declined.

Figures (6) – (9) depict the effects of a material parameter upon temperature, concentration and angular velocity. Figure (6) delineates the influence of material parameters upon velocity distribution. This is evident that an increased in material parameter as a result the dimensionless velocity distribution are higher. Figure (7) illustrate the influence of material parameters upon velocity distribution. This is clear that an increased in material parameter as a result the angular velocity distribution are higher. Figure (8) elucidate that temperature is affected by material parameters. It is clear that as a material parameters value increased, the temperature distribution decreased. Figure (9) delineate the concentration distributions from the curves it is visible that the material parameters increased as a result the dimensionless concentration distribution are lower.

Figure (10) depicts the effects of the Prandtl number upon the dimensionless concentration distributions from curves depict that the Prandtl number increased as a result the dimensionless temperature distribution is reduced. Figure (11) demonstrates the Eckert numbers effects on temperature. It is clear from the graphs that as the Eckert numbers rise, temperature decreases. Figure (12) illustrate that the dimensionless concentration distributions are decreasing and the Schmidt numbers have increased. Figure (13) describe that a thermophoresis parameter effects on concentration. The rise in the thermophoresis parameter is attributed to rise in concentration profile. Figure (14) describe that a thermophoresis parameter effects on concentration. It is explicitly stated that the concentration distributions are decreasing and the Brownian motion parameter is increasing.

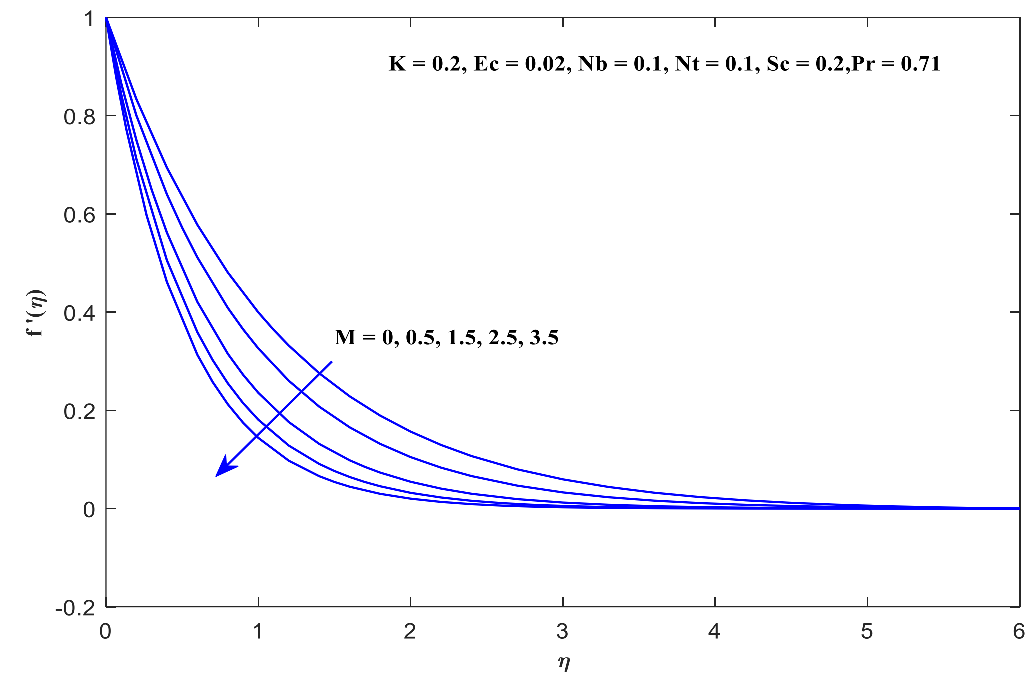

Figure 2. Velocity profile for magnetic number *M*.

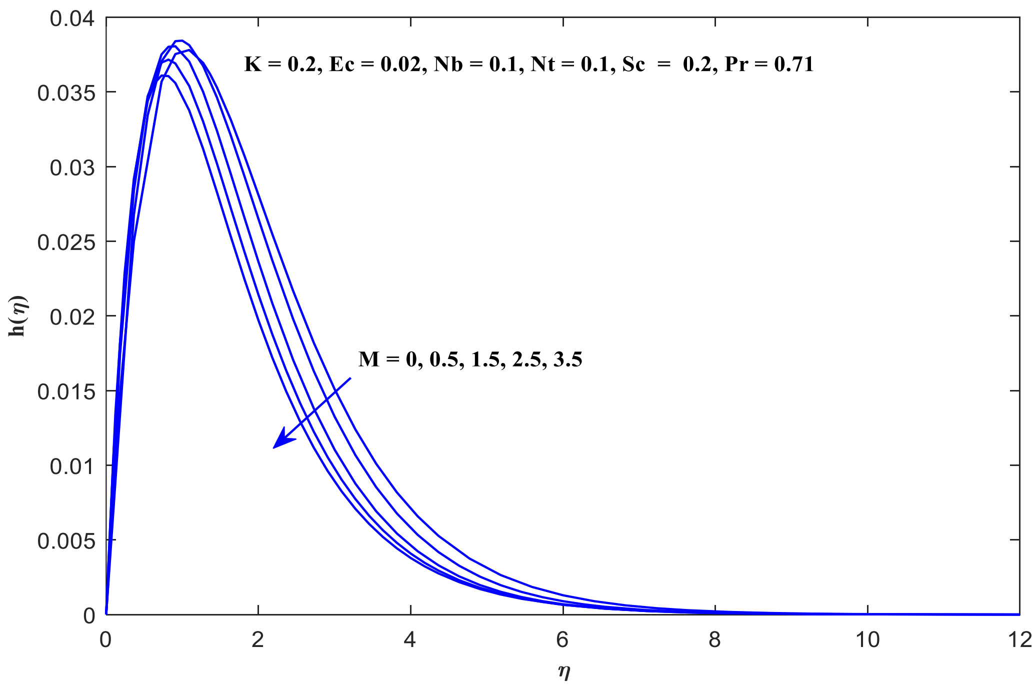

Figure 3. Angular velocity profile for magnetic number *M*.

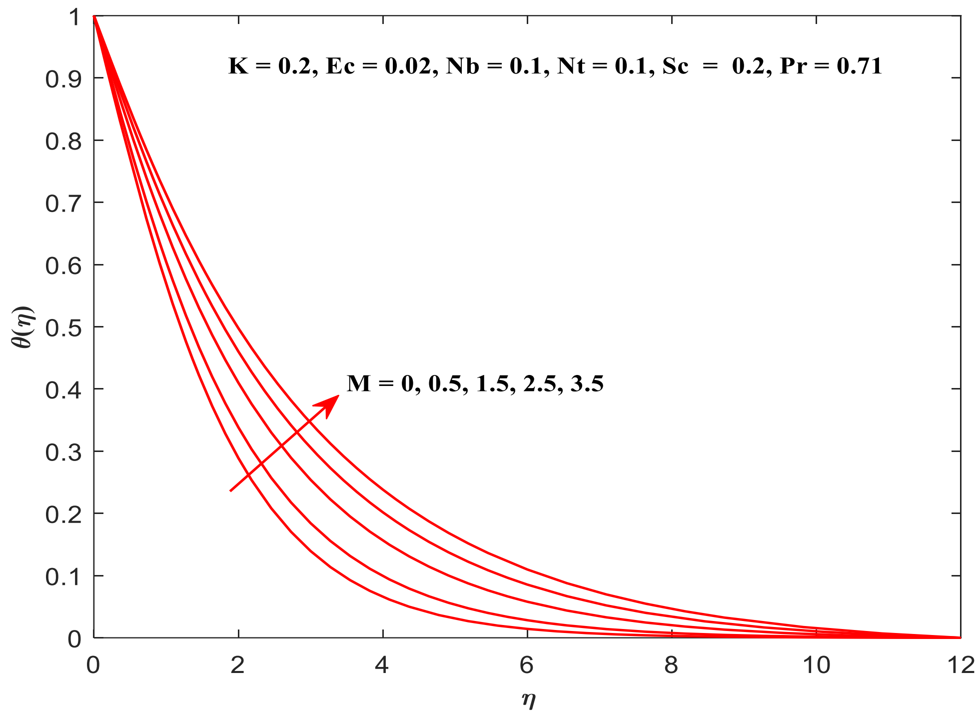

Figure 4. Temperature profile for Magnetic number *M*.

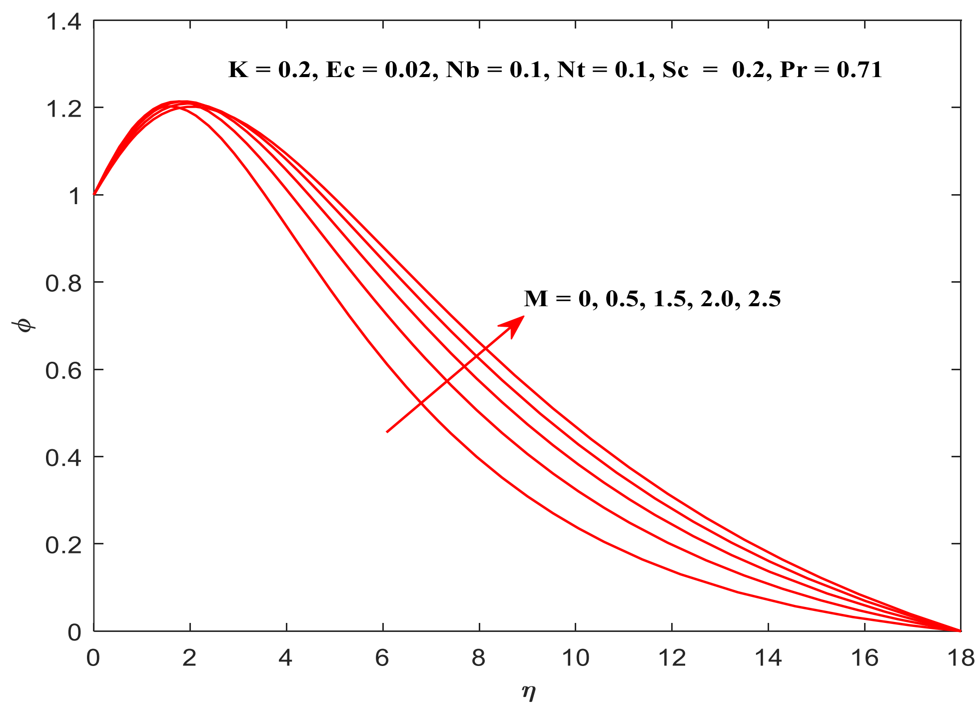

Figure 5. Concentration profile for magnetic number *M*.

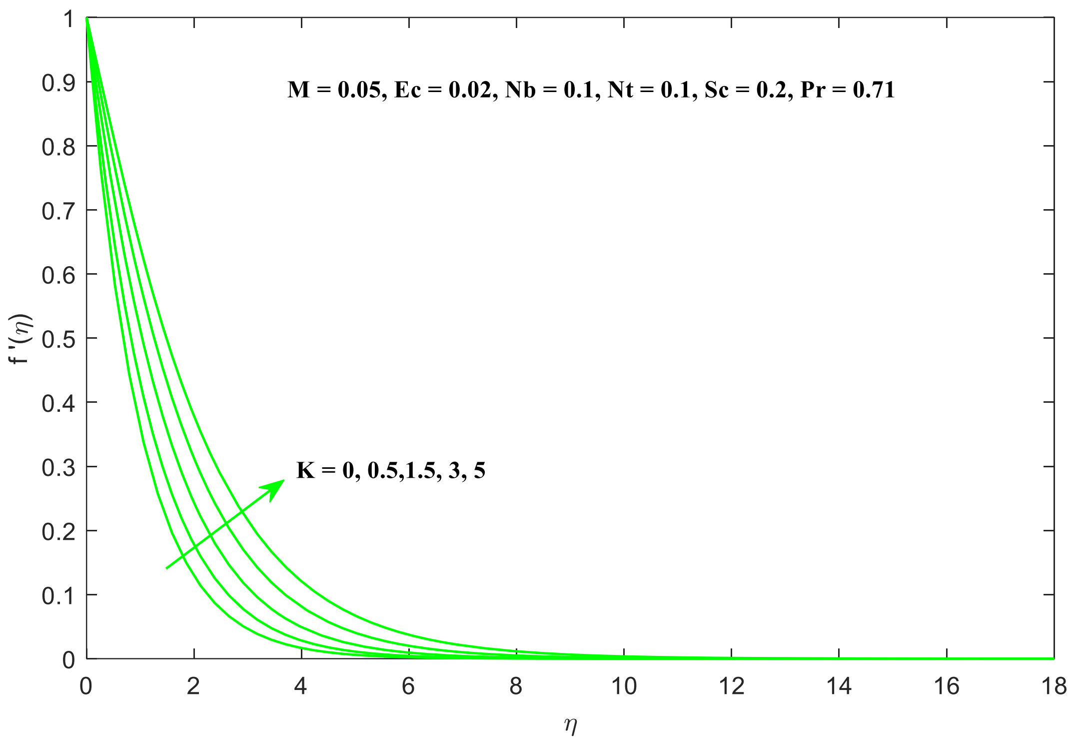

Figure 6. Effects of material number *K* on Velocity profile.

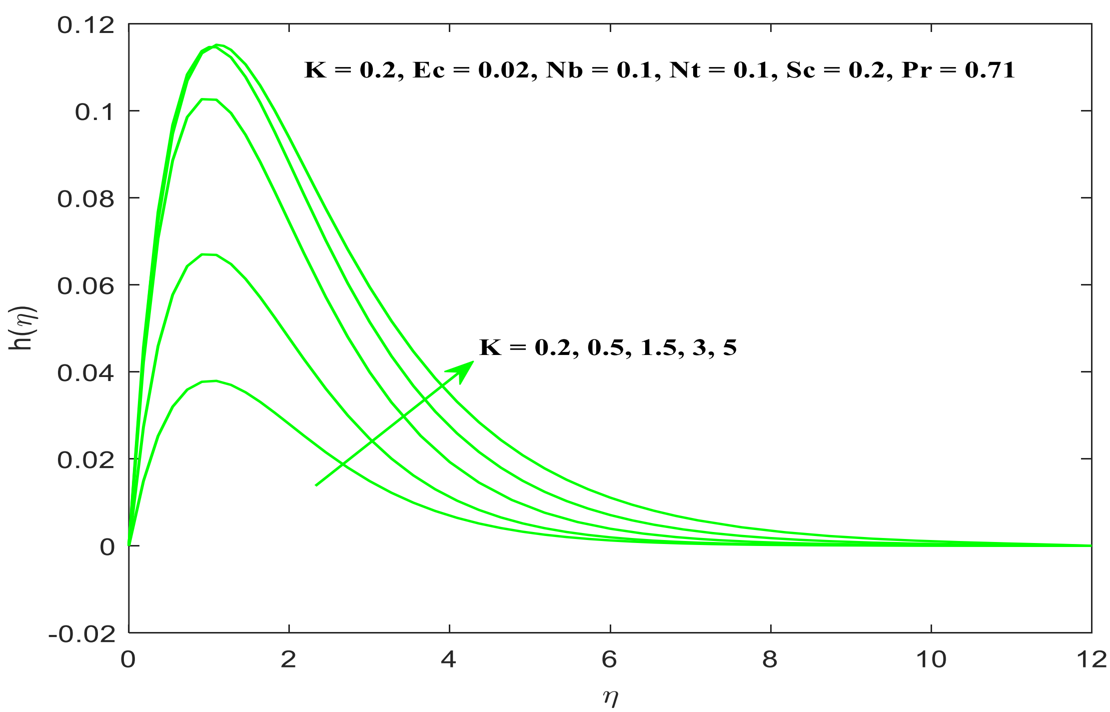

Figure 7. Effects of material number *K* on Angular velocity profile.

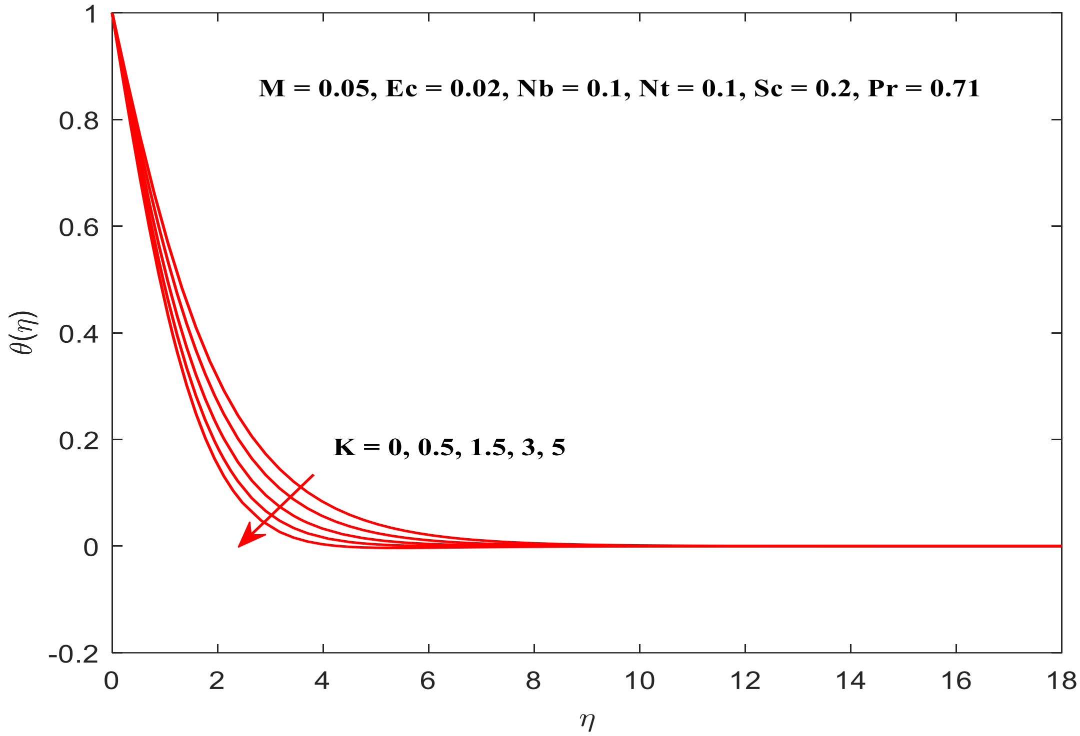

Figure 8. Effects of material number *K* on Temperature profile.

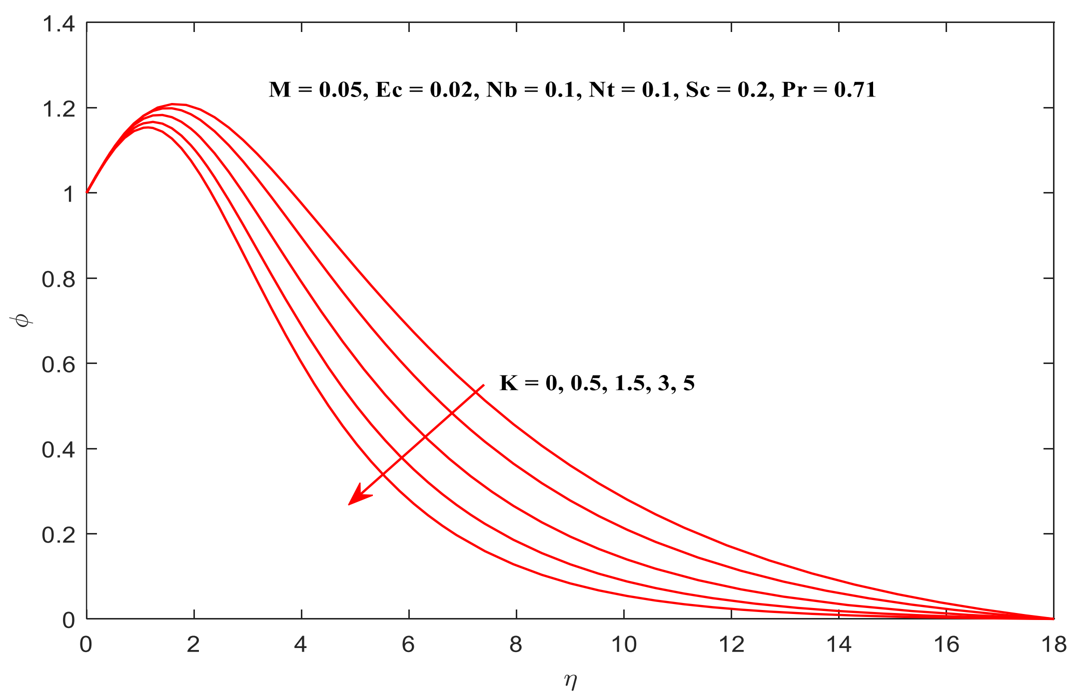

Figure 9. Effects of material number *K* on Concentration profile.

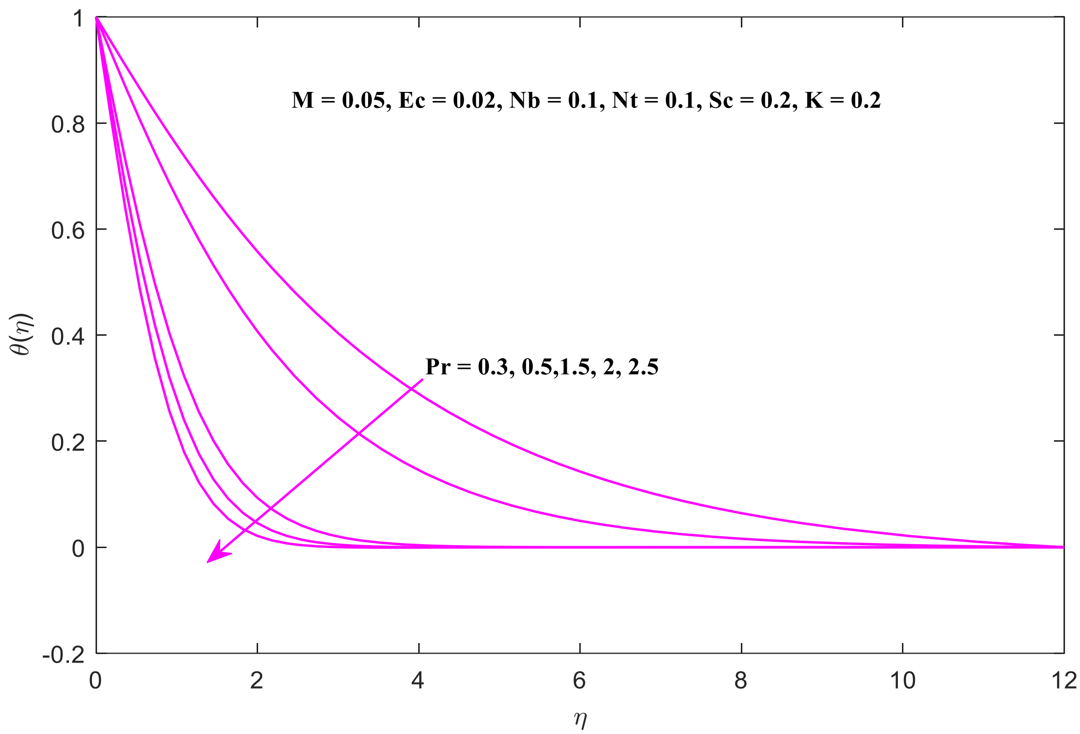

Figure 10. Effects of Prandtl number *Pr* on Temperature profile.

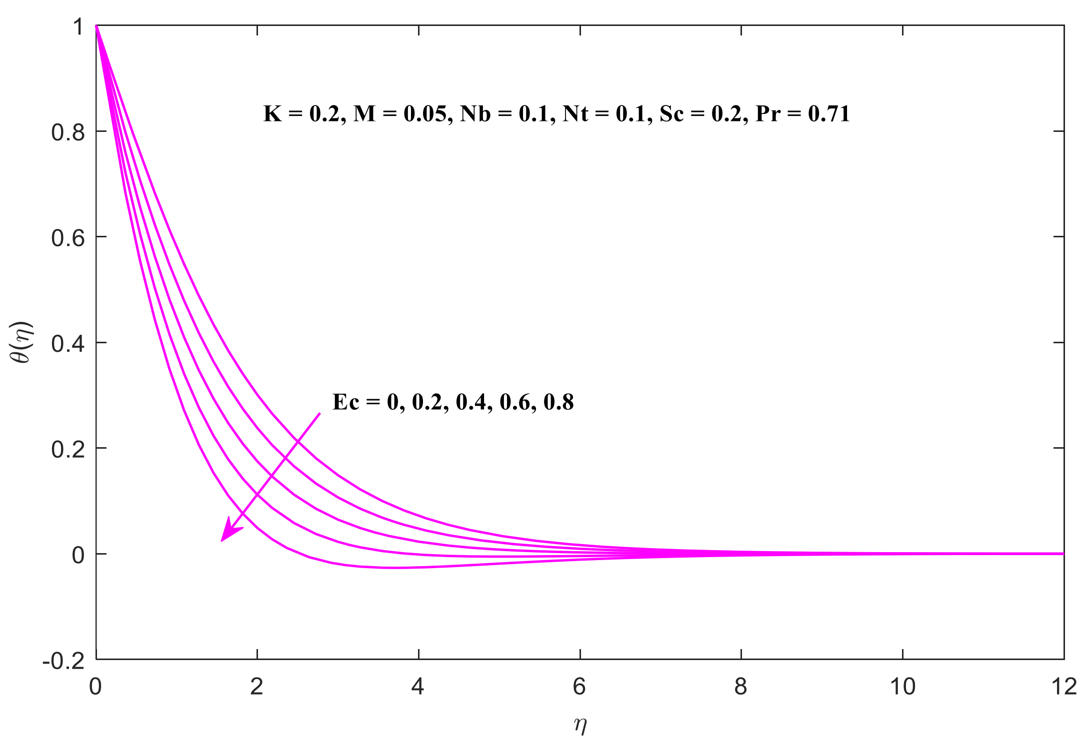

Figure 11. Effects of Eckert number *Ec* on Temperature profile.

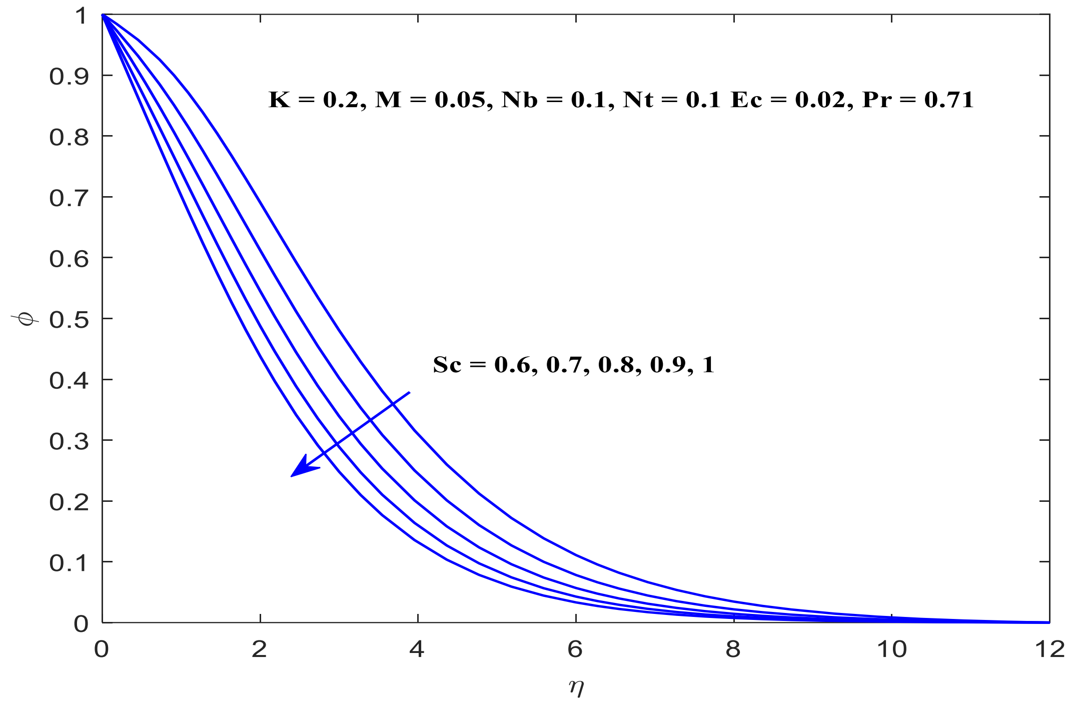

Figure 12. Variation of *Sc* on Concentration profile.

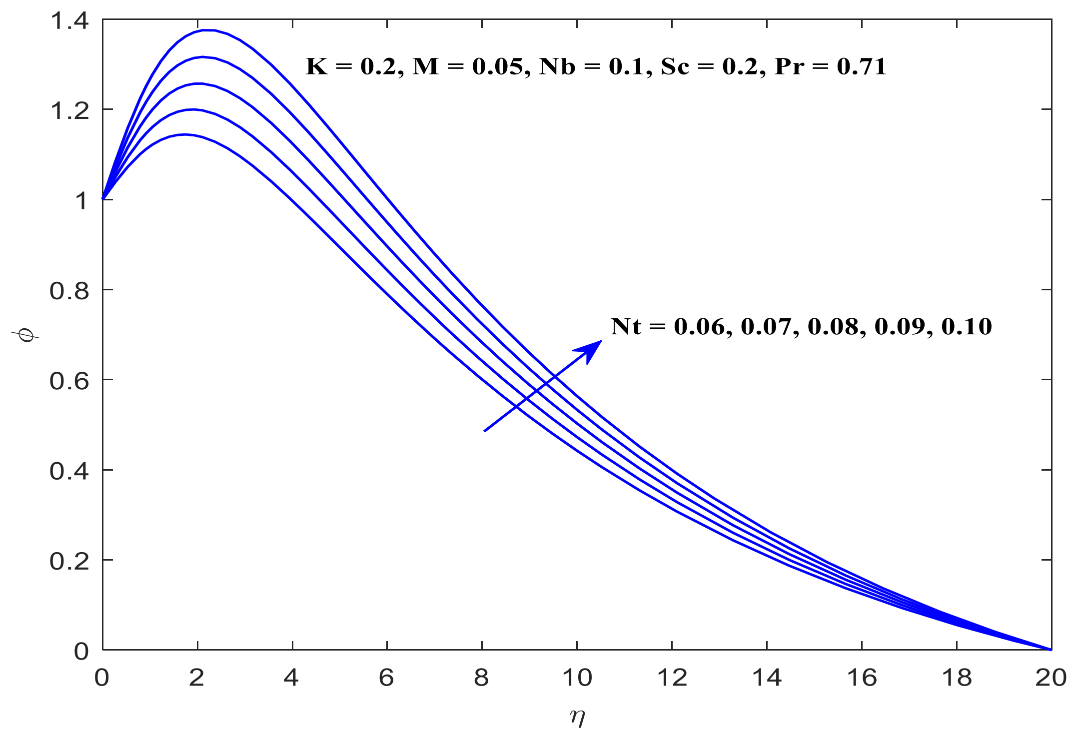

Figure 13. Variation of *Nt* on Concentration profile.

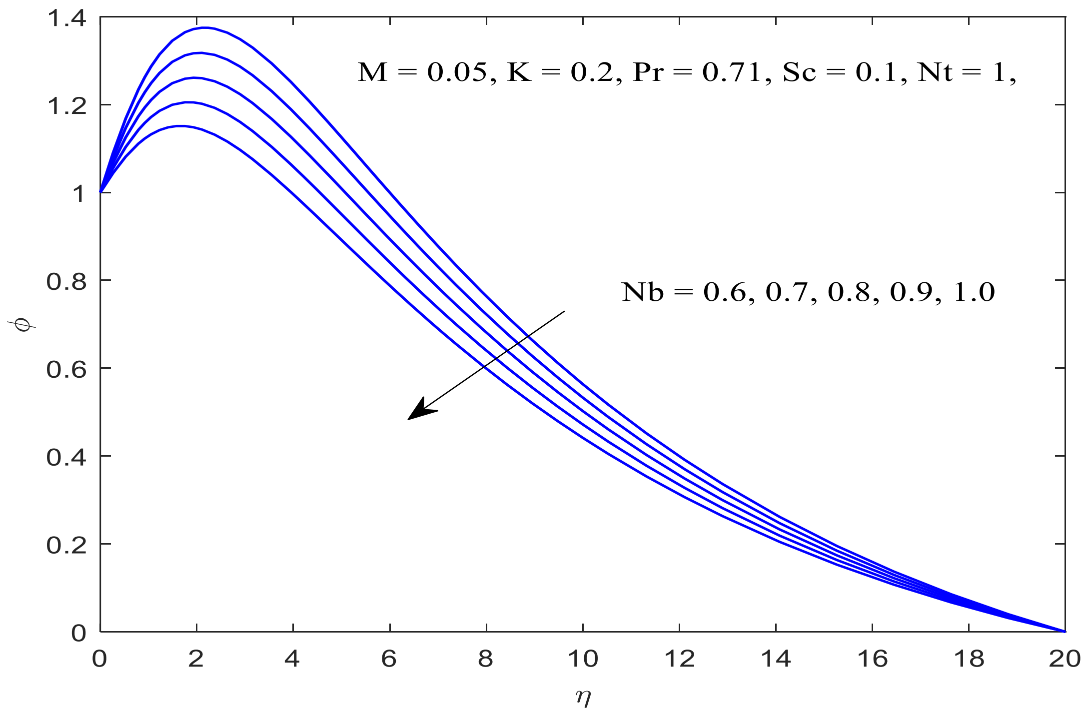

Figure 14. Variation of *Nb* on Concentration profile.

CHAPTER 4

MICROPOLAR FLUID FLOW WITH ZERO MASS FLUX OF NANOPARTICLES IN A POROUS MEDIUM

This chapter is continuation of the previous chapter by adding some new effects and constraints. There has been a comprehensive investigation of heat transfers of Micropolar by considering porous medium and heat absorption. Subsequently, mathematical formulation was modeled using boundary conditions. Using similarity variables, for a formal formulation, all PDEs for such governing equations of momentum, energy, angular momentum and concentration are converted into nonlinear ODEs. At the end, nonlinear ODEs are solved by using MATLAB to get closed solution.

4.1 Mathematical Formulation of the problem

In this problem, we are considering cartesian coordinate system with a moving surface incompressible, stationary, two-dimensional, micropolar, and nano-fluid laminar flow. The governing equations that represent boundary layer flow for equations of continuity, momentum, angular momentum, energy, and concentration can be defined by using the approximate boundary conditions:

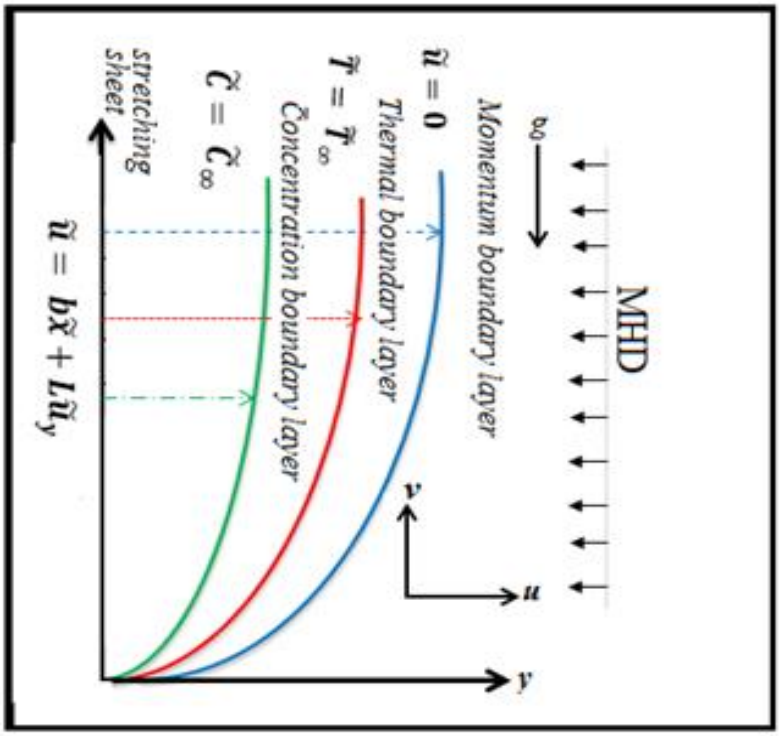

Figure 15. Geometry of problem

$$\frac{\partial \tilde{u}}{\partial x} + \frac{\partial \tilde{v}}{\partial y} = 0, \tag{4.1}$$

$$\rho\left(\tilde{u}\ \frac{\partial \tilde{u}}{\partial x} + \tilde{v}\ \frac{\partial \tilde{u}}{\partial y}\right) = (\mu + \kappa)\left(\frac{\partial^2 \tilde{u}}{\partial y^2}\right) + \kappa\left(\frac{\partial \widetilde{N}}{\partial y}\right) - \sigma B_0^2\ \tilde{u} + \frac{\nu}{\kappa}\tilde{u}$$

$$\pm g[\beta_T(T - T_\infty) + \beta_c(C - C_\infty)], \tag{4.2}$$

$$\rho j\left(\tilde{u}\ \frac{\partial \widetilde{N}}{\partial x} + \tilde{v}\frac{\partial \widetilde{N}}{\partial y}\right) = \gamma\frac{\partial^2 \widetilde{N}}{\partial x^2} + \kappa\left(\frac{\partial \widetilde{N}}{\partial y} + 2\widetilde{N}\right), \tag{4.3}$$

$$\rho C_p\left(\tilde{u}\frac{\partial \tilde{T}}{\partial x} + \tilde{v}\ \frac{\partial \tilde{T}}{\partial y}\right) = k\left(\frac{\partial^2 \tilde{T}}{\partial y^2}\right) + (\mu + \kappa)\left(\frac{\partial \tilde{u}}{\partial y}\right)^2 + \sigma B_0^2\ \tilde{u}^2 + \frac{(\rho Cp)_p}{(\rho Cp)_f}\left[D_B\frac{\partial C}{\partial y}\frac{\partial \tilde{T}}{\partial y} + \right.$$

$$\left.\frac{D_T}{D_B}\left(\frac{\partial \tilde{T}}{\partial y}\right)^2\right] + \frac{Q_0}{\rho C_p}(\bar{T} - \bar{T}_\infty), \tag{4.4}$$

$$\tilde{u}\frac{\partial \tilde{C}}{\partial x} + \tilde{v}\frac{\partial \tilde{C}}{\partial y} = D_B\frac{\partial^2 \tilde{C}}{\partial y^2} + \frac{D_T}{T_\infty}\frac{\partial^2 \tilde{T}}{\partial y^2}, \tag{4.5}$$

Boundary conditions take the following way:

$$\tilde{u} = bx + L\frac{\partial \tilde{u}}{\partial y}, \tilde{v} = 0, \quad \tilde{N} = 0, \quad \tilde{T} = \tilde{T}_w, \ \tilde{C} = \tilde{C}_w, \quad as \ \ \tilde{y} = 0 \tag{4.6a}$$

$$\tilde{u} = 0, \tilde{N} = 0, \ \tilde{T} = \tilde{T}_\infty \ , \ \tilde{C} = \tilde{C}_\infty \ , \qquad as \ \ \tilde{y} \rightarrow \infty \tag{4.6b}$$

By introducing the similarity transformation:

$$\tilde{\eta} = \sqrt{b/\nu_f}\ \tilde{y}, \tilde{u} = b\tilde{x}\, f'(\eta), \tilde{v} = -\sqrt{b\nu_f} f(\eta), \ \tilde{N} = \sqrt{b^3/\nu_f}\,\tilde{x} g(\eta), \tag{4.7a}$$

$$\tilde{\theta}(\eta) = \frac{\tilde{T}-\tilde{T}_\infty}{\tilde{T}_w-\tilde{T}_\infty}, \ \tilde{T} = \tilde{T}_\infty + A\tilde{x}\theta(\eta), \ \tilde{\phi}(\eta) = \frac{\tilde{C}-\tilde{C}_\infty}{\tilde{C}_w-\tilde{C}_\infty}, \ \tilde{C} = \tilde{C}_\infty + B\tilde{x}\phi(\eta), \tag{4.7b}$$

Stream function ψ can be expressed as:

$$\tilde{u} = \tilde{\psi}_y \ , \quad \tilde{v} = -\tilde{\psi}_x \ . \tag{4.7c}$$

Making use of these transformations, identically continuity equation is satisfied and equation (4.2 – 4.5) along with the conditions on boundary (4.7a) and $(4.7b)$ takes the following expressions:

$$(1+K)f''' + ff'' - f'^2 + Kg' - Mf' + \frac{1}{D_a}f' \pm Gr_1\theta \pm Gr_2\phi = 0, \tag{4.8}$$

$$(1+K/2)g'' + fg' - f'g - K(2g + f'') = 0, \tag{4.9}$$

$$\theta'' + Prf\theta' - Prf'\theta + (1+K)PrEcf''^2 + PrEcMf'^2 + PrNb\theta'\emptyset' + PrNt\theta'^2 + PrQ\theta = 0, \tag{4.10}$$

$$\phi'' + Scf\phi' - Scf'\phi + \frac{N_t}{N_b}\theta'' = 0, \tag{4.11}$$

Where,

$Gr_1 = \frac{G_r}{Re_x^2}$ is the thermal buoyancy parameter and $Gr_2 = \frac{G_c}{Re_x^2}$ is the buoyancy parameter.

$G_r = \frac{g\beta_t\,(\tilde{T}_w - \tilde{T}_\infty)\,x^3}{\nu^2}$ is the local Grashof number and $G_c = \frac{g\beta_c\,(\tilde{C}_w - \tilde{C}_\infty)\,x^3}{\nu^2}$ is the local solutal Grashof number.

$Da = \frac{\kappa b}{\nu}$, $Q = \frac{Q_0}{k_f(\rho c_p)_f b}$, $K = \frac{\kappa}{\mu}$, $Pr = \frac{c_p \mu}{\kappa}$, $M = \frac{\sigma B_0^2}{\rho b}$, $Ec = \frac{\tilde{u}^2}{c_\rho(\tilde{T}_w - \tilde{T}_\infty)}$,

$N_b = \frac{(\rho Cp)_p \, D_B \, (\tilde{C}_w - \tilde{C}_\infty)}{(\rho Cp)_f \, \nu_f}$, $N_t = \frac{(\rho Cp)_p \, D_T \, (\tilde{T}_w - \tilde{T}_\infty)}{(\rho Cp)_f \, \nu_f \, \tilde{T}_\infty}$

By using similarity transformations (4.7a) and (4.7b), Conditions (4.6a) and (4.6b) takes the following form:

$$f(\eta) = 0, \; f'(\eta) = 1 + sf''(\eta), \; \theta(\eta) = \phi(\eta) = 1 \qquad at \;\; \eta = 0 \tag{4.12a}$$

$$f'(\eta) = g(\eta) = \theta(\eta) = \phi(\eta) = 0 \qquad as \;\; \eta \to \infty \tag{4.12b}$$

Surface flux is defined by:

$$\tilde{q}_w(x) = -k_f \left(\frac{\partial \tilde{T}}{\partial y}\right)_{y=0} = -k_f (\tilde{T}_w - \tilde{T}_\infty) \sqrt{\frac{b}{\nu_f}} \theta'(0), \tag{4.13}$$

The surface heat flux transfer coefficient can be expressed as:

$$\tilde{h}(x) = \frac{\tilde{q}_w(x)}{(\tilde{T}_w - \tilde{T}_\infty)}, \tag{4.14}$$

$$\tilde{\tau}_w = (k + \mu)_f b \tilde{x} \sqrt{\frac{b}{\nu_f}} \, f''(0), \tag{4.15}$$

The physical quantities of interest are skin friction coefficient, the local Nusselt number, and the local Sherwood number, which are defined by

$$C_f = \frac{\tilde{\tau}_w}{\rho_f \tilde{u}_w^2}$$

Putting Eq. (4.7a) and (4.7 b) into Eq. (4.13) and (4.15), we get

$$C_f \sqrt{\tilde{R}e_w} = (1 + \tilde{K}) \, |f''(0)|, \tag{4.16}$$

Nusselt number can be defined by

$$\tilde{N}u_x = \frac{\tilde{x} \tilde{h}(x)}{k_f(\tilde{T}_w - \tilde{T}_\infty)},$$

or

$$\tilde{N}u_x = \frac{\tilde{x} \tilde{h}(x)}{k_f} = -\sqrt{\frac{b}{\nu_f}} \tilde{x} \theta'(0), \tag{4.17}$$

or

$$\frac{\tilde{N}u_x}{\sqrt{Re_w}} = -\theta'(0)\,,$$

Sherwood number can be defined as

$$\tilde{S}h_x = \; -\sqrt{\frac{b}{v_f}}\,\tilde{x}\phi'(0), \tag{4.18}$$

or

$$\frac{\tilde{S}h_x}{\sqrt{Re_w}} = \; -\phi'(0),$$

4.2 Methodology

By employing the built-in bvp4c approach after conversion of the given PDEs to the first order ODEs using MATLAB program for the solution, Consider:

$f = y_1,$ $g = y_4$ $\theta = y_6,$ $\phi = y_8,$

$f' = y_2,$ $g' = y_5$ $\theta' = y_{7,}$ $\phi' = y_9,$

$f'' = y_3,$ $g'' = y_{11}$ $\theta'' = y_{12},$ $\phi'' = y_{13},$

$f''' = y_{10},$

$$Eq(4.8) \Longrightarrow (1+K)y_{10} + y_1y_2 - y_2^2 + Ky_5 - My_2 + \frac{1}{D_a}y_2 \pm Gr_1y_6 \pm Gr_2y_8 = 0,$$

$$\Rightarrow y_{10} = \frac{1}{1+K}\left[-y_1y_2 + y_2^2 - Ky_5 + My_2 - \frac{1}{D_a}y_2 \pm Gr_1y_6 \pm Gr_2y_8\right], \quad (4.19)$$

$$Eq(4.9) \Longrightarrow \left(1+\frac{K}{2}\right)y_{11} + y_1y_5 - y_2y_4 - K(2y_4 + y_3) = 0,$$

$$\Rightarrow y_{11} = 2\left(\frac{-y_1y_5 + y_2y_4 + K(2y_4 + y_3)}{2+K}\right), \quad (4.20)$$

$$Eq(4.10) \Longrightarrow \quad y_{12} + Pry_1y_7 + (1+K)PrEcy_3^2 + PrEcMy_2^2 + PrN_by_7y_9 + PrN_ty_7^2 + PrQy_6 = 0,$$

$$\Longrightarrow y_{12} = -Pry_1y_7 - (1+K)PrEcy_3^2 - PrEcMy_2^2 - PrN_by_7y_9 - PrN_ty_7^2 - PrQy_6, \quad (4.21)$$

$$Eq(4.11) \Longrightarrow y_{13} + Scy_1y_9 - Scy_2y_8 + \frac{N_t}{N_b}y_{12} = 0$$

$$\Rightarrow y_{13} = -Scy_1y_9 + Scy_2y_8 - \frac{N_t}{N_b}y_{12}, \quad (4.22)$$

$$\Rightarrow \begin{bmatrix} f' \\ f'' \\ f'' \\ f''' \\ g' \\ g'' \\ \theta' \\ \theta'' \\ \phi \\ \phi'' \end{bmatrix} = \begin{bmatrix} y_2 \\ y_3 \\ y_{10} \\ y_5 \\ y_{11} \\ y_7 \\ y_{12} \\ y_9 \\ y_{13} \end{bmatrix} \begin{bmatrix} y_2 \\ y_3 \\ \left(\dfrac{-y_1 y_2 + y_2^2 - K y_5 + M y_2 - \dfrac{1}{D_a} y_2 \pm Gr_1 y_6 \pm Gr_2 y_8}{1 + K} \right) \\ y_5 \\ 2\left(\dfrac{-y_1 y_5 + y_2 y_4 + K(2y_4 + y_3)}{2 + K} \right) \\ y_{11} \\ -Pr y_1 y_7 - (1 + K) Pr Ec y_3^2 - Pr Ec M y_2^2 - Pr Nb y_7 y_9 - Pr N_t y_7^2 - Pr Q y_6 \\ y_9 \\ -Sc y_1 y_9 + Sc y_2 y_8 - \dfrac{N_t}{N_b} y_{12} \end{bmatrix}$$

4.3 Results and discussion

For the sake of require results for the above boundary value problems. We first transformed all the PDEs of momentum, angular momentum, energy and concentration into non-linear ODEs by similarity transformation with their corresponding boundary conditions. One very interesting behavior is observed that the energy equation is being transformed into two cases. The first solution associated with positive (+) part of the eq. (4.8) represents assisting flow while second solution associated with negative (−) part of eq. (4.8) represents opposing flow. The results of these two cases are shown in graphs where solid line indicates assisting flow while dotted lines indicates opposing flow. The effects are apparent for all physical parameters involved and the nonlinear ODEs are illustrated to velocity profile, temperature profile, angular velocity profile, and concentration profiles. The impacts for some of parameters are seen in graphs where the arrows in the figure indicates the increasing and decreasing in assisting flow and opposing flow.

Figures (16) – (19) demonstrate the fluctuation of velocity profile, angular velocity profile, temperature profile and concentration profiles variation on magnetic parameter for both assisting and opposing flow. Figure (16) demonstrates that Lorentz force, which decreases the velocity profile for both assisting and opposing flows, causes resistance in the path of fluid flow as a result of the influence of the magnetic field. The impact of magnetic number on angular velocity is seen in Figure (17). This is evident that by larger values of magnetic number may lower angular velocity profile for both assisting and opposing flows. In Figure (18) It has been observed that increasing values of M corresponding to increasing temperature distributions. Higher values of M produce a resistive type of force on the motion, reacting in the reverse direction of motion and decreasing the velocity field as a result. The fluid motion simultaneously produced some thermal energy, increasing the fluid temperature for assisting and opposing flows. Figure (19) illustrate the effect of magnetic number on concentration profile and variation in magnetic number may affect both solutions as a result concentration profile is observed to decrease as M rises.

Figures (20) – (23) Show that changes in the material parameter cause changes in the velocity profile, angular velocity profile, temperature profile, and concentration profile. Figure (20) and (21) illustrates that K varies with velocity and angular velocity profile, respectively. As a result, angular velocity and velocity are increased for assisting and opposing flows and Figure (22) and (23) shows the reverse behavior. The temperature profile and concentration profile decrease as K increases.

Figure (24) shows the fluctuation of the temperature profile is examined for Prandtl numbers. The curves clearly show the increase in Pr causes a lower in temperature. Figure (25) demonstrates that raising Eckert number Ec leads into a decline in temperature on both assisting and opposing flows. Figure (26) illustrate the impact of Schmidt numbers upon concentration profile, the curves show that as Schmidt numbers increase, the concentration profile becomes lower. Figure (27) and (28) represents the variation in the concentration profiles of *Nt* and *Nb*. For assisting and opposing flows, concentration rises as the thermophoresis parameter increase and decreasing for the values of the Brownian motion increase.

Figures (28) – (33) depict the variations in skin-friction, the Nusselt number and the Sherwood number for different values of Eckert number, magnetic number, Brownian motion number, thermophoresis parameter, microrotation and Schmidt number. From Figures (28) – (33) shows that with increasing values of *M*, *Ec, Nb*, *Nt* and *n*, the Skin friction increased and also Nusselt and Sherwood number increased.

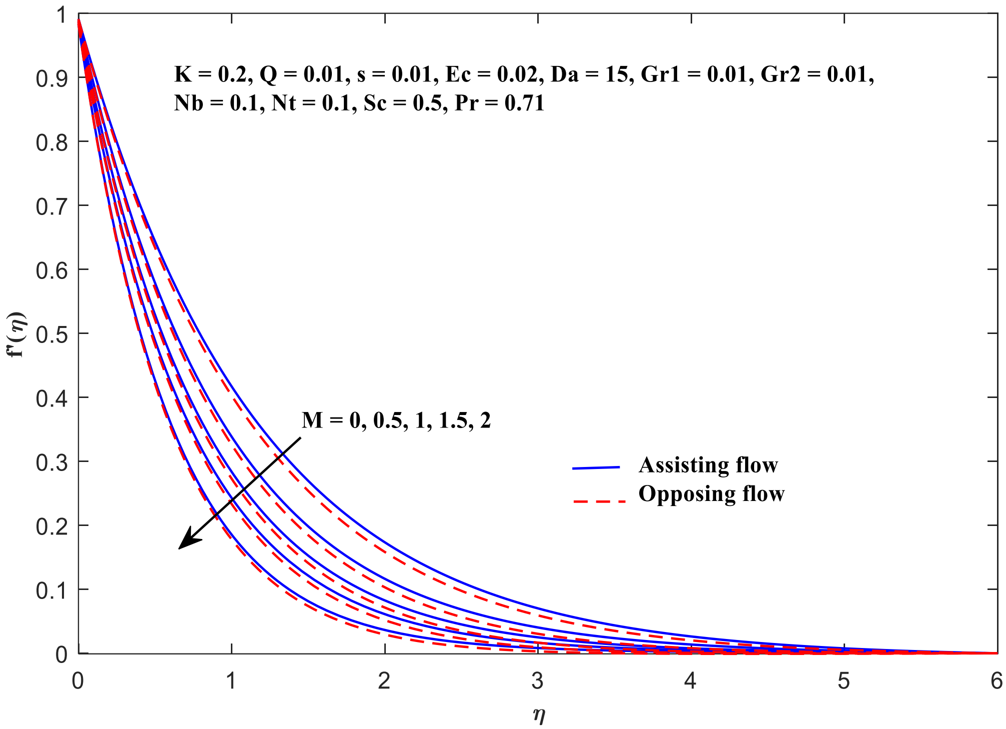

Figure 16. Effects of magnetic number *M* on Velocity profile.

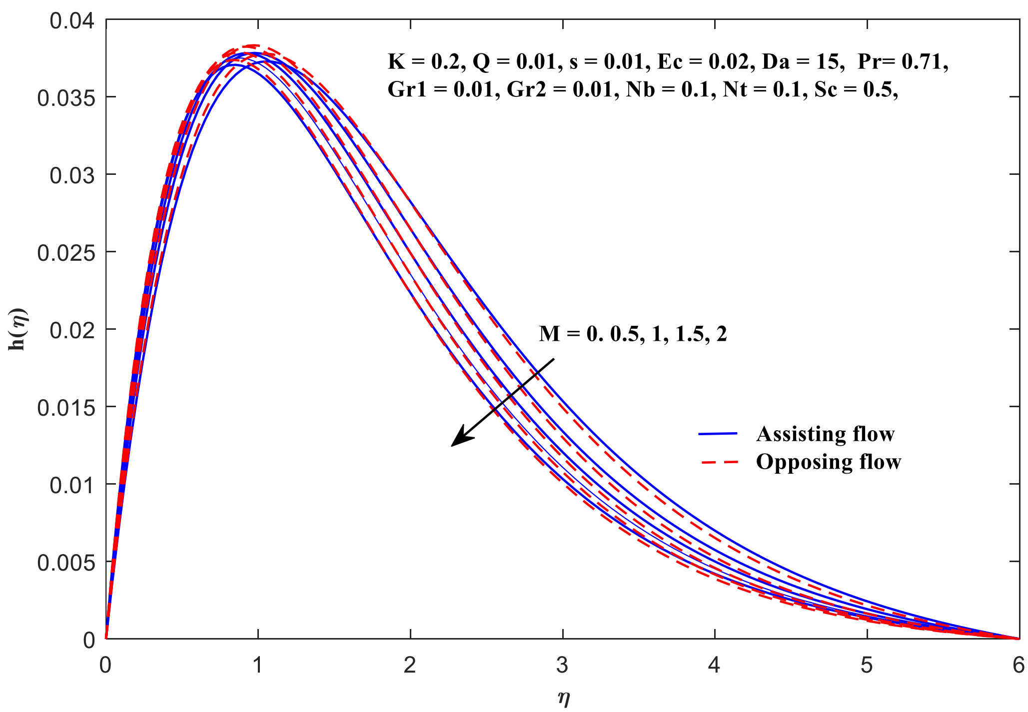

Figure 17. Effects of magnetic number *M* on Angular velocity profile.

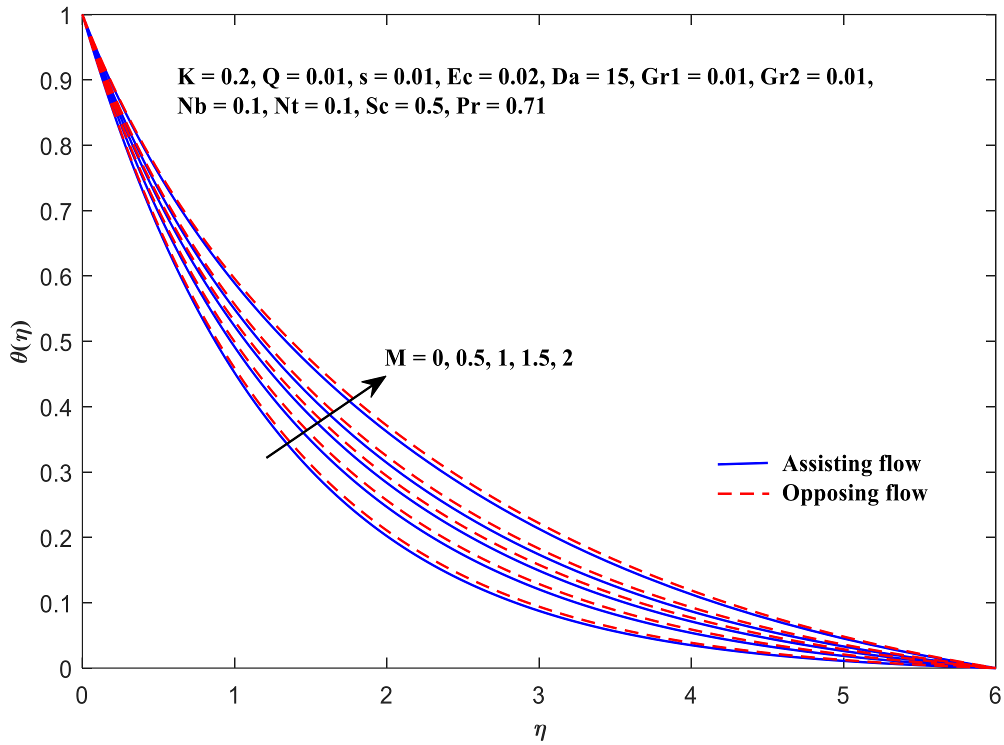

Figure 18. Effects of magnetic number *M* on temperature profile.

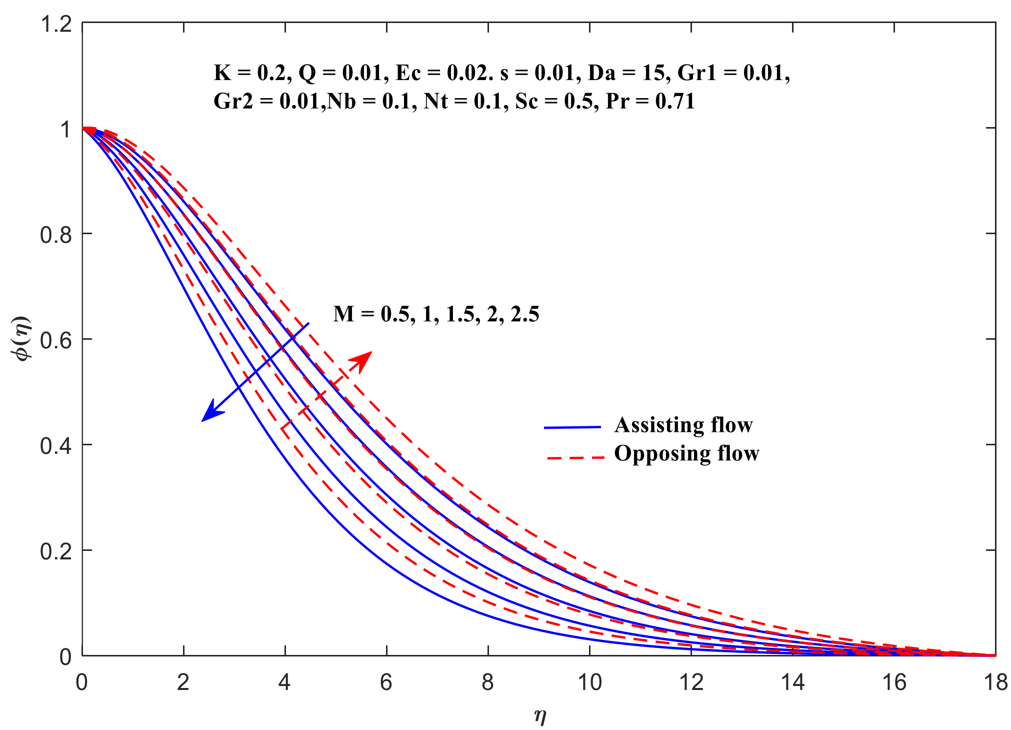

Figure 19. Effects of magnetic number *M* on concentration profile.

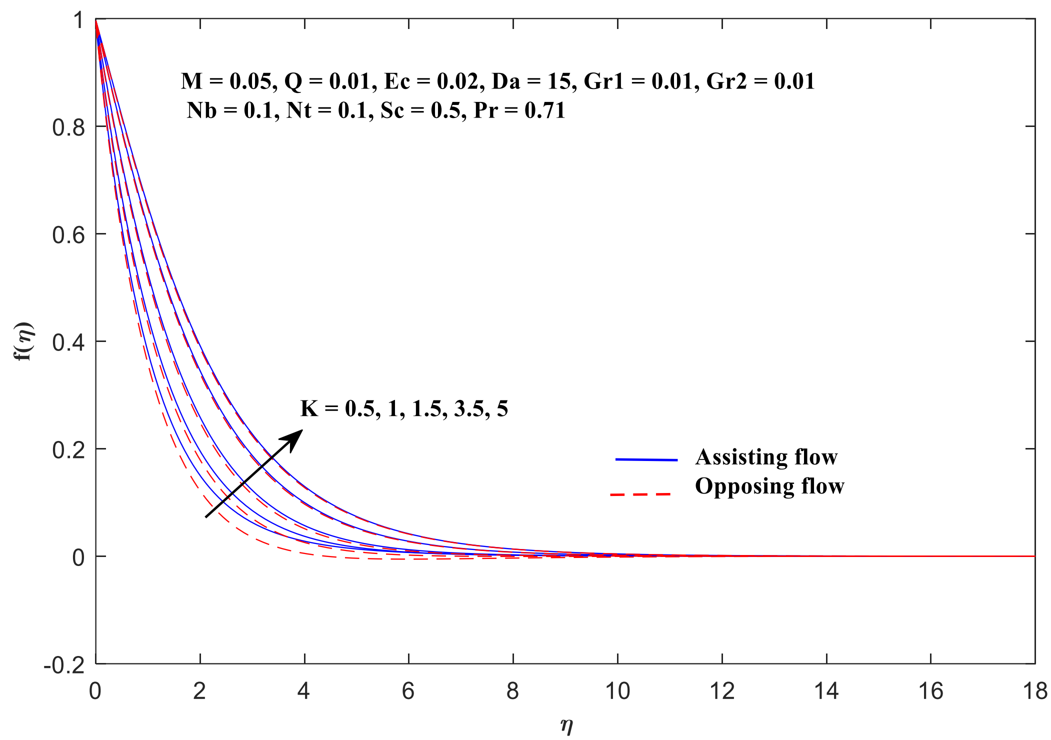

Figure 20. Effects of material number K on velocity profile.

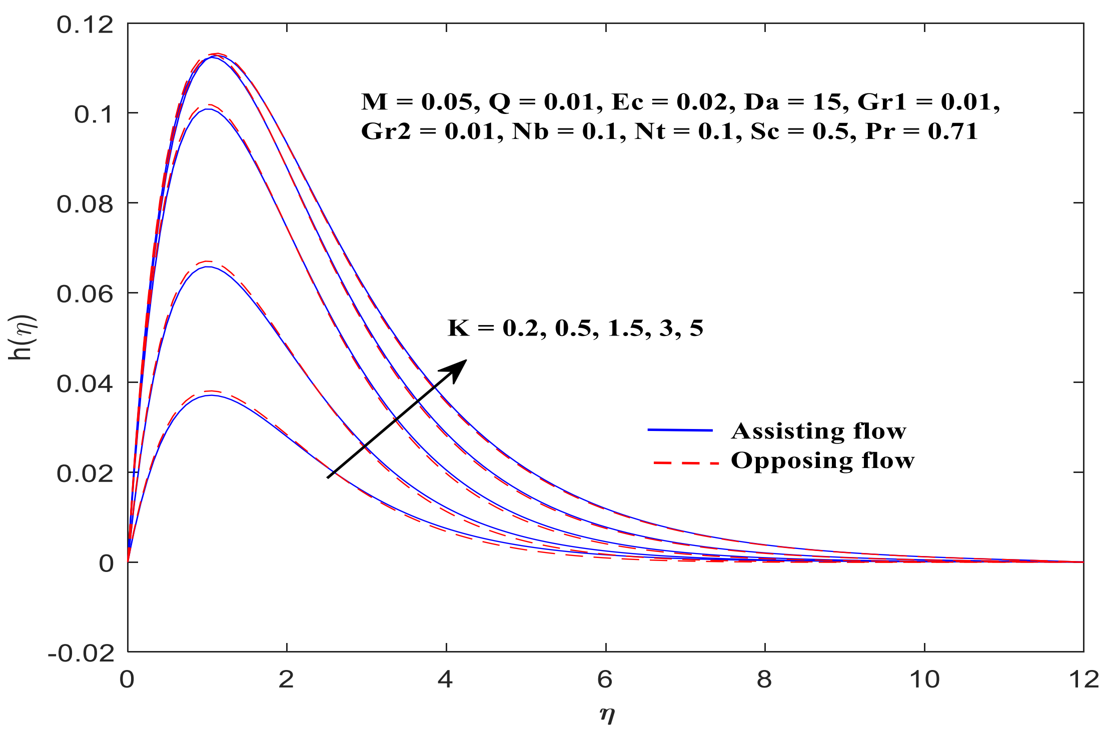

Figure 21. Effects of material number K on Angular velocity profile.

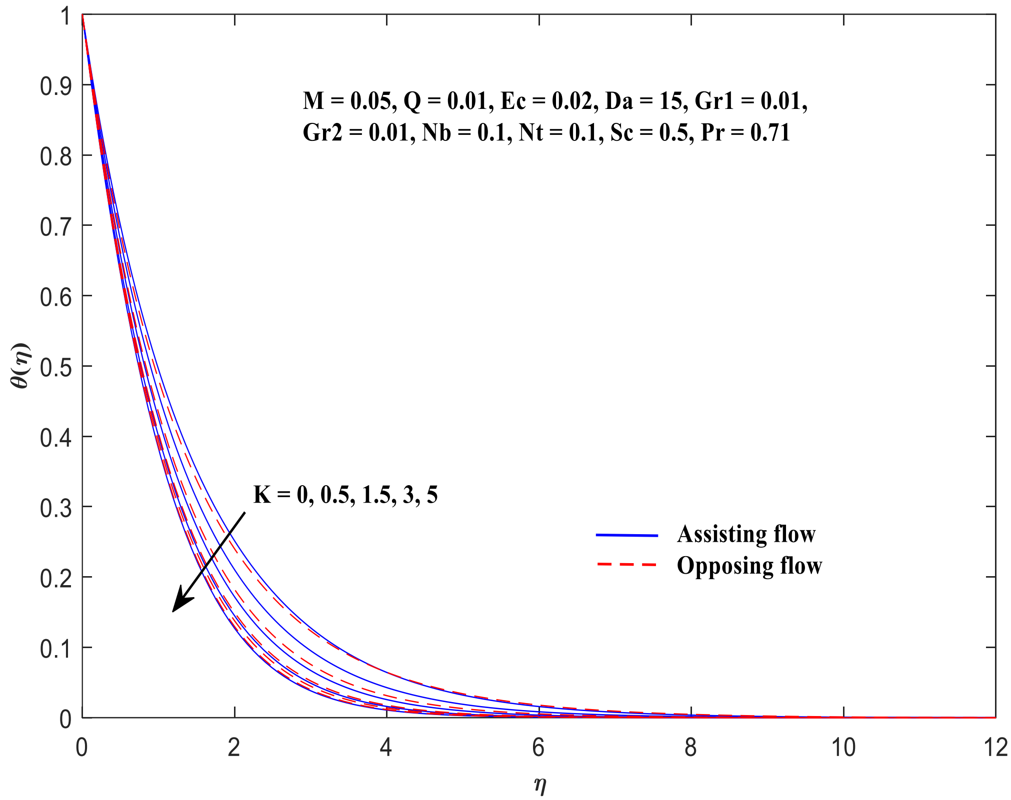

Figure 22. Effects of material number *K* on Temperature profile.

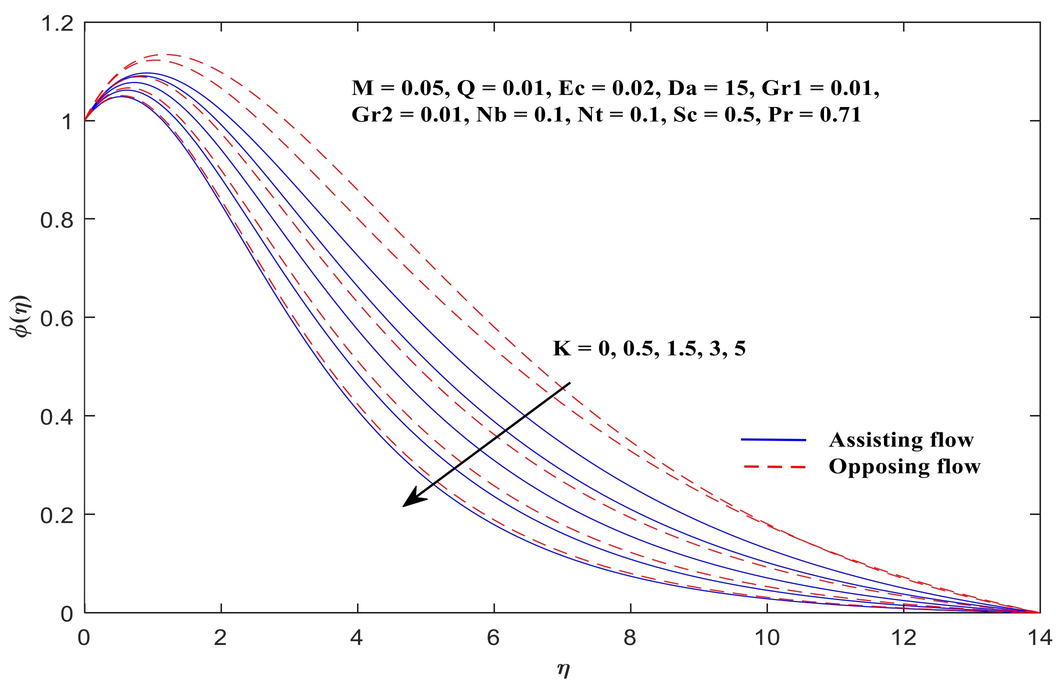

Figure 23. Effects of material number *K* on Concentration profile.

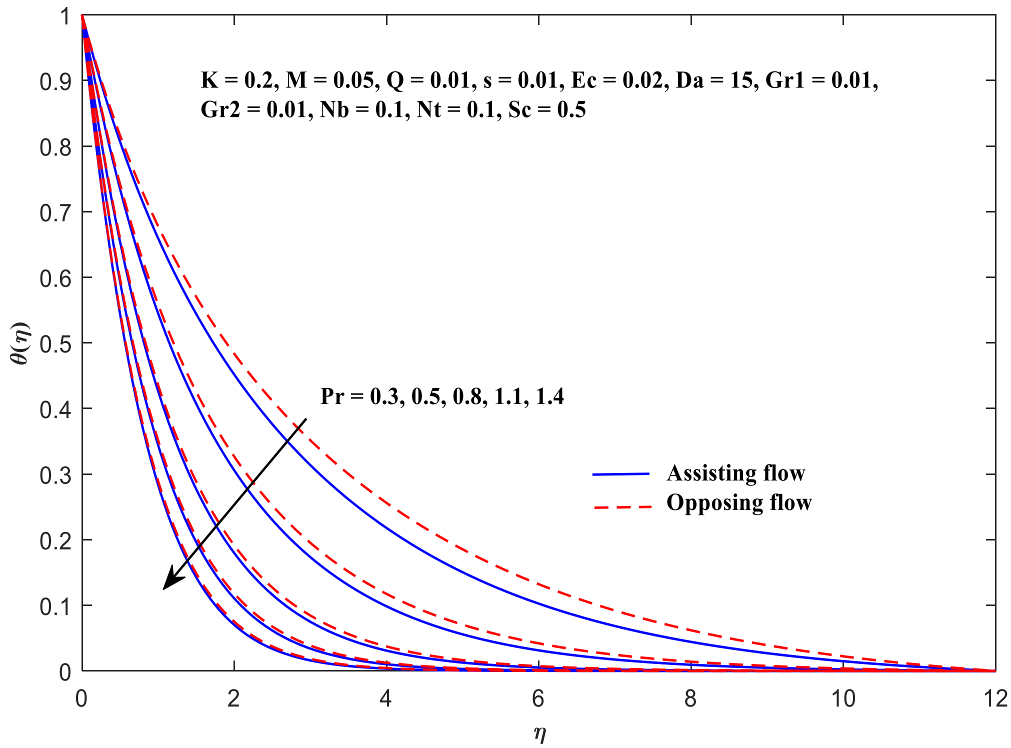

Figure 24. Effects of Prandtl number *Pr* on Temperature profile.

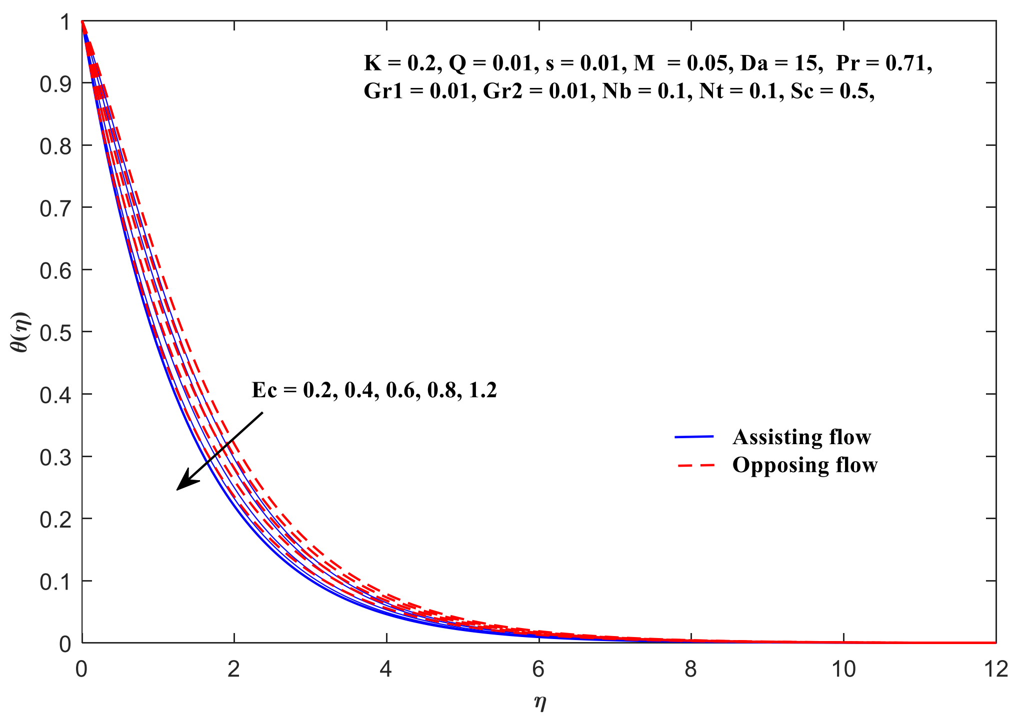

Figure 25: Effects of Eckert number *Ec* on Temperature profile.

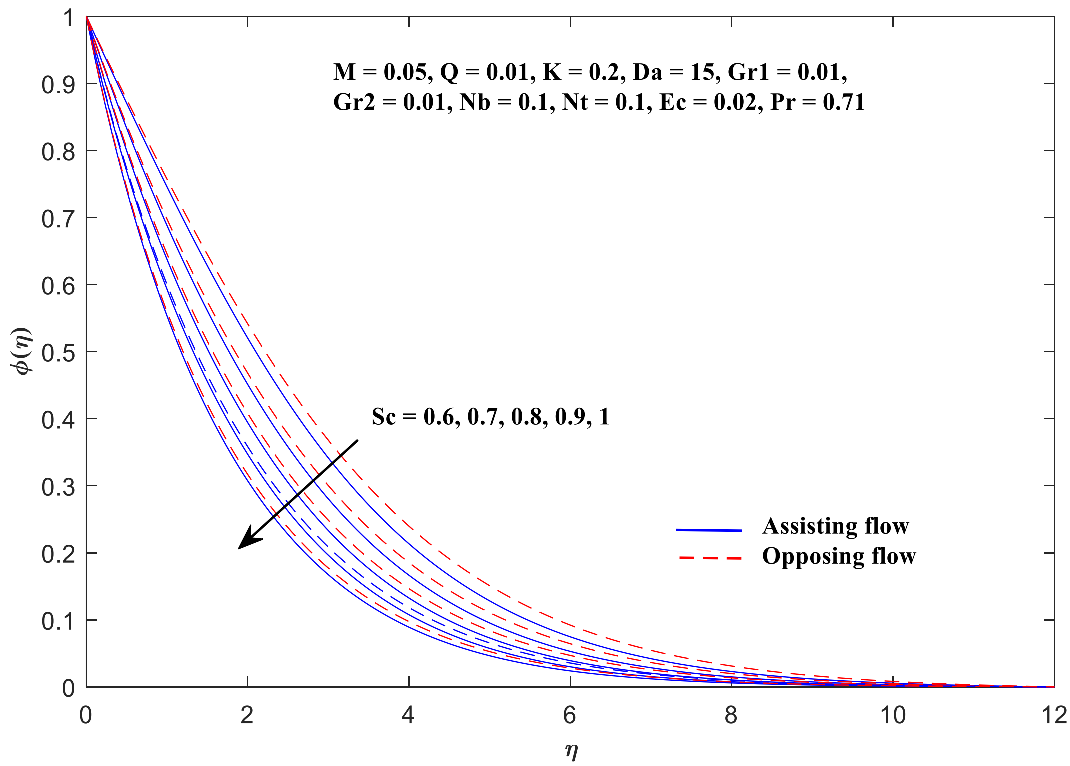

Figure 26.Variation of *Sc* on Concentration profile.

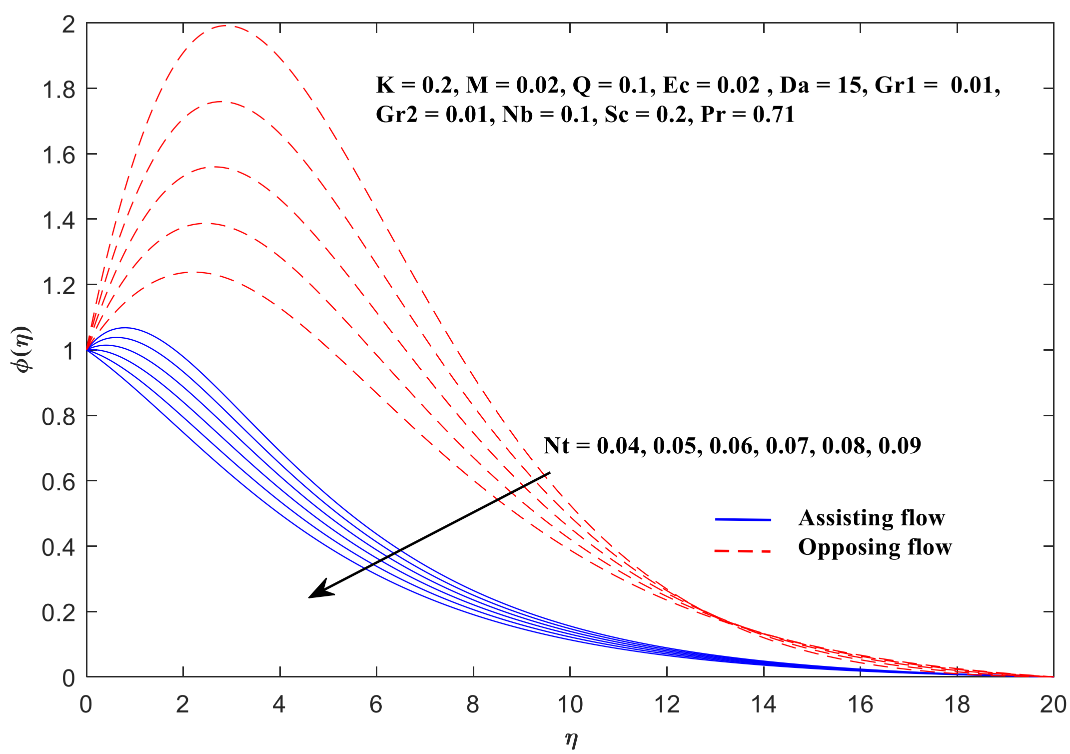

Figure 27. Variation of *Nt* on Concentration profile.

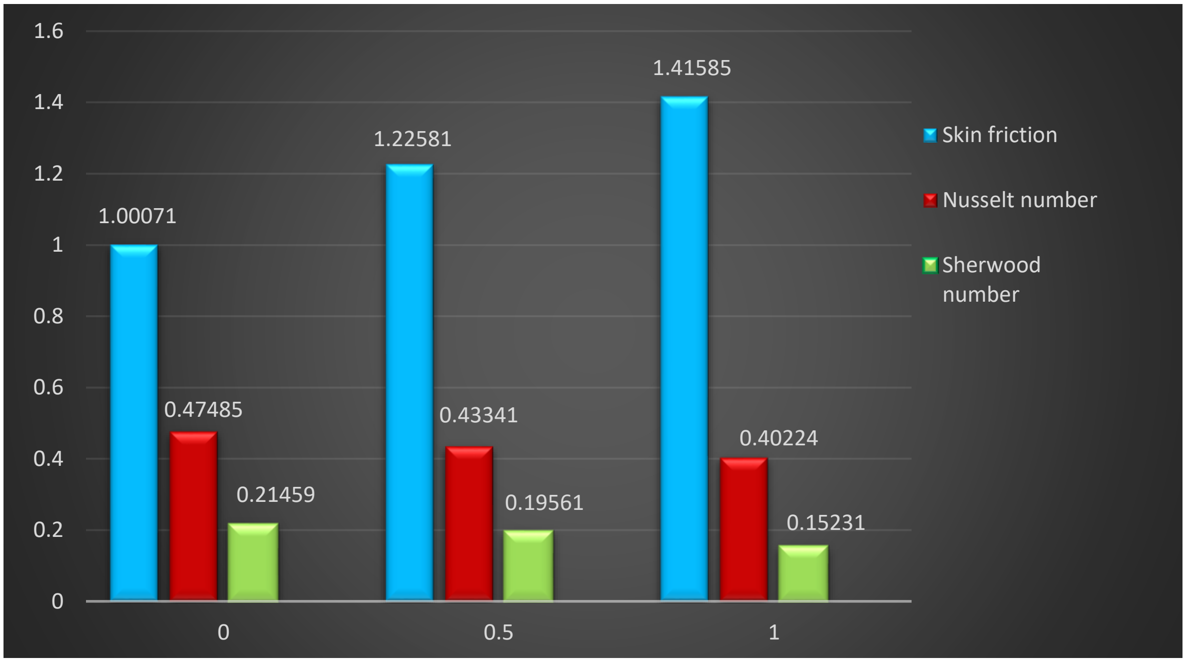

Figure 28. Variation in skin-friction, Nusselt number and Sherwood number for various values of *M*.

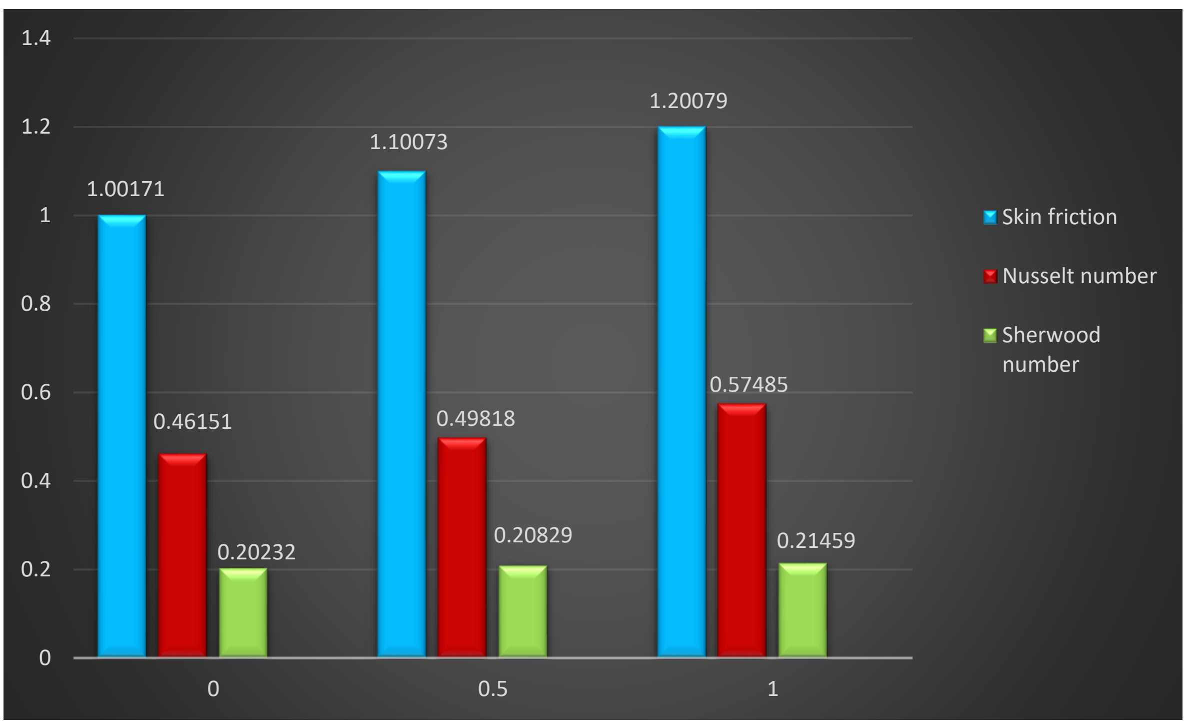

Figure 29. Variation in skin-friction, Nusselt number and the Sherwood number for various values of *Ec*.

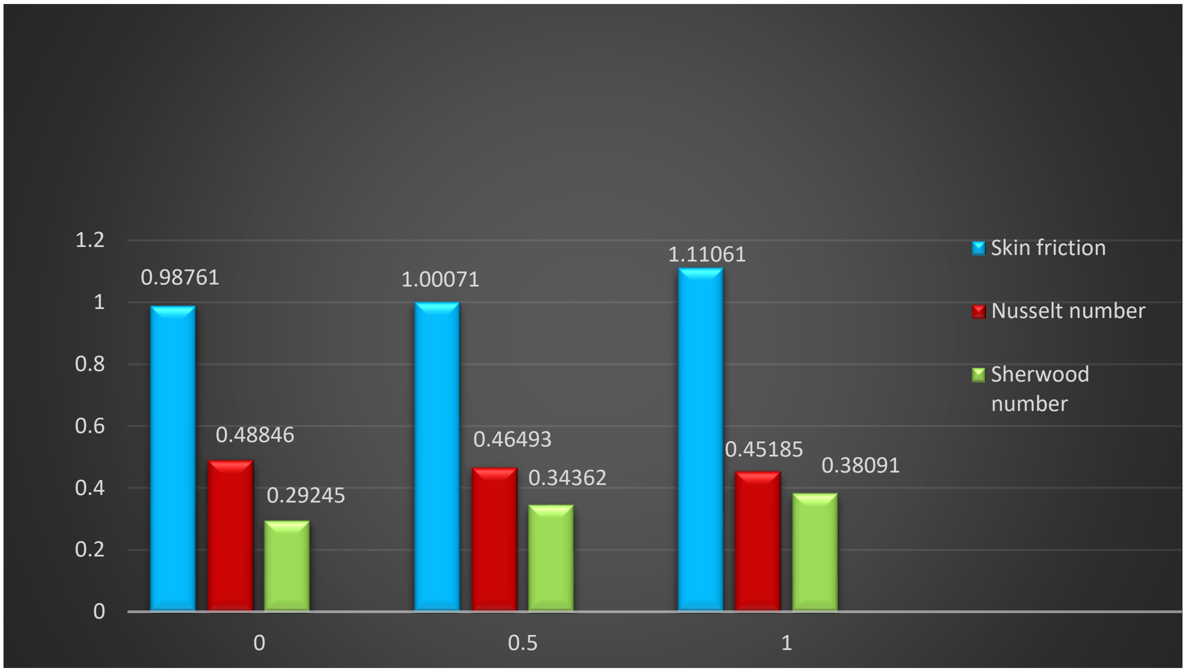

Figure 30. Variation in skin-friction, Nusselt number and Sherwood number for various values of *Nb*.

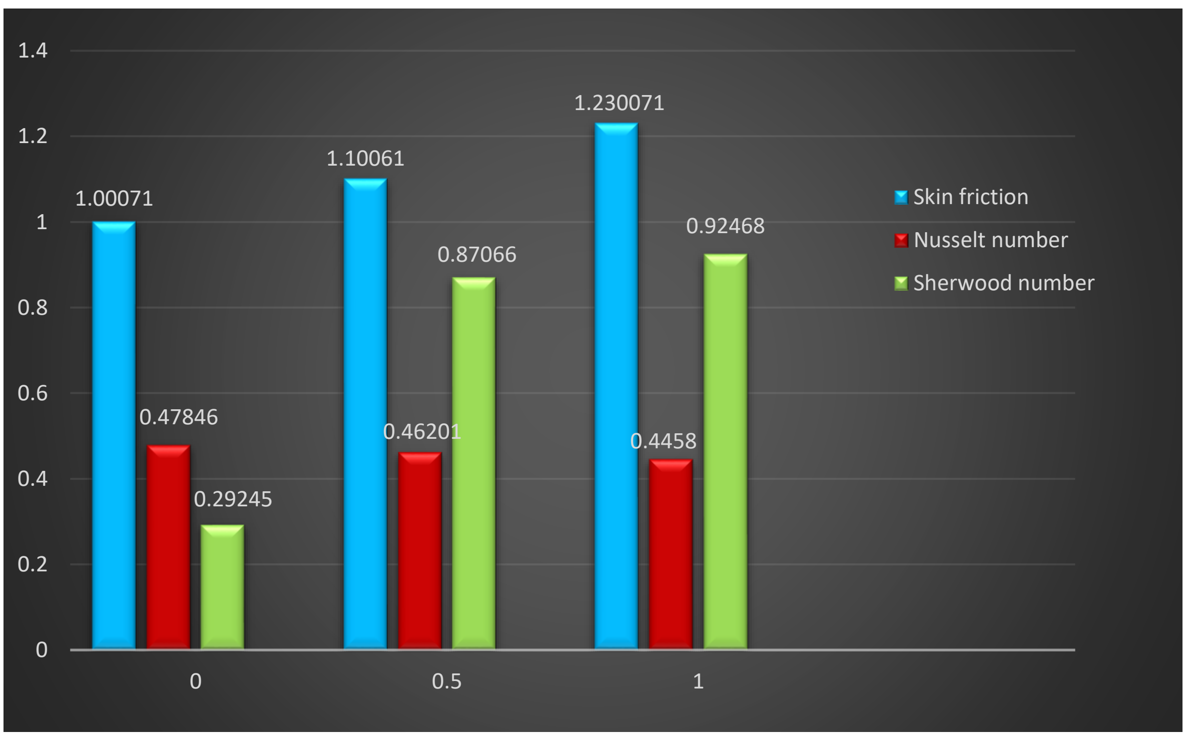

Figure 31. Variation in skin-friction, Nusselt number and Sherwood number for various values of *Nt*.

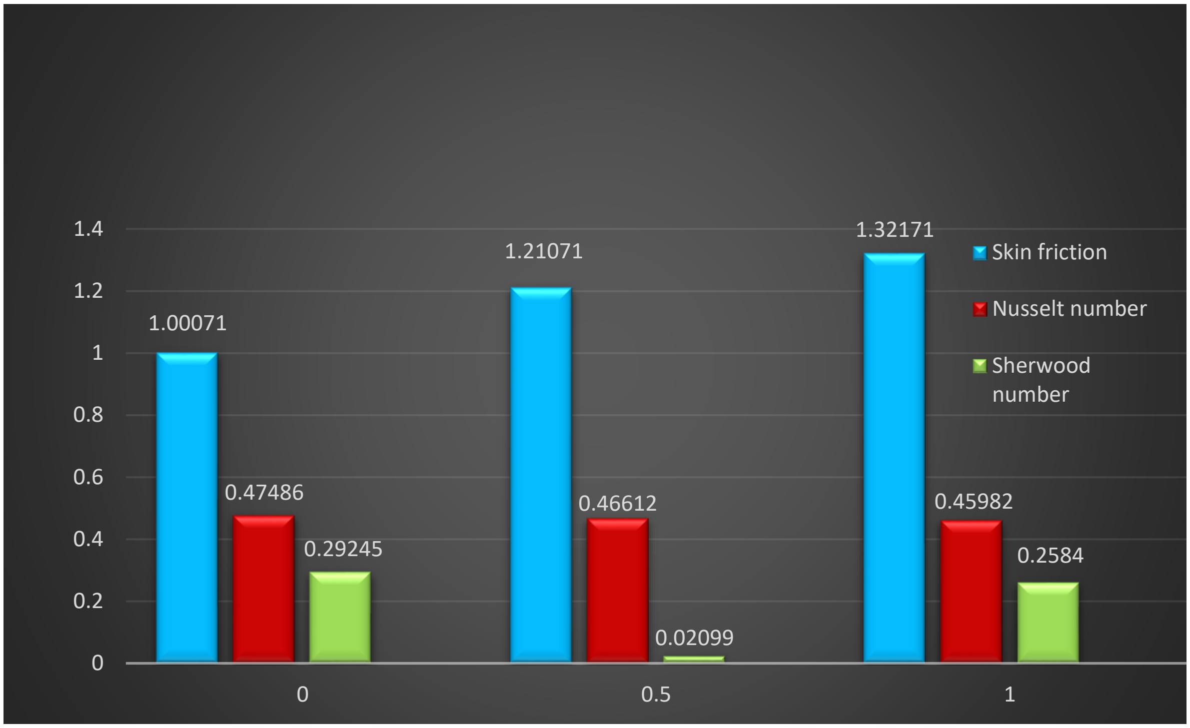

Figure 32. Variation in skin-friction, Nusselt number and Sherwood number for various values of *Sc*.

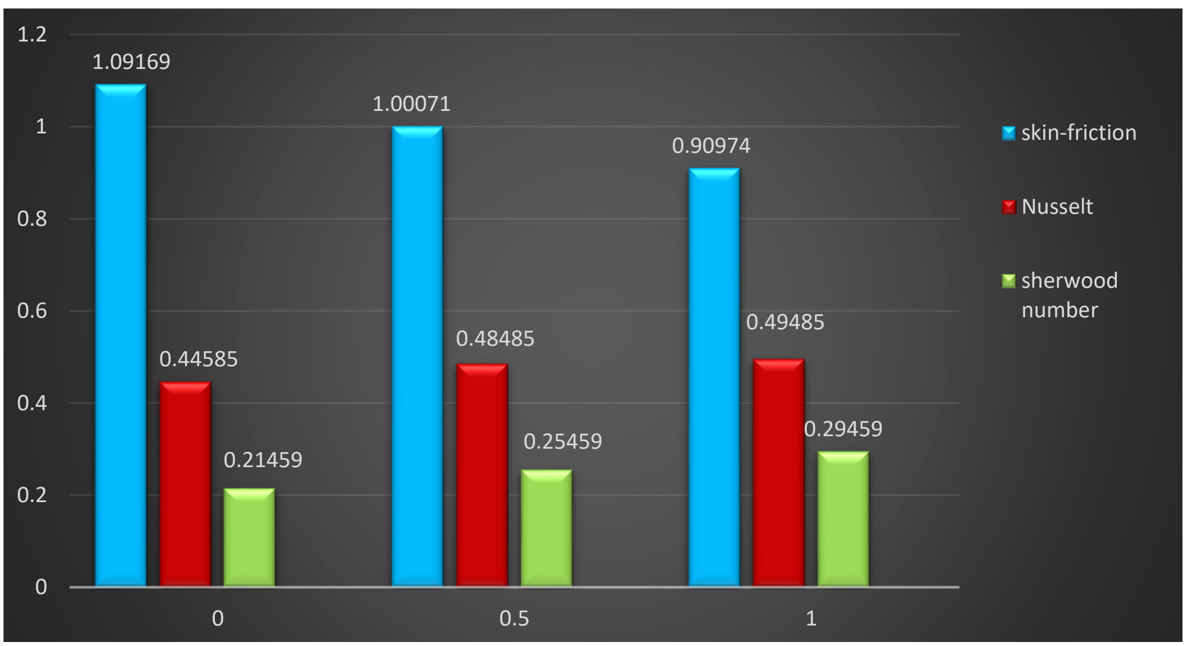

Figure 33. Variation in skin-friction, Nusselt number and Sherwood number for various values of *n*.

CHAPTER 5

CONCLUSION

Initially, an article has been reviewed and formulated its mathematical equations. The parameters obtained from these equations were shown graphically using MATLAB. At the end a thorough discussion on results and graphs are upheld.

Addition of some new parameters in review article took place in an extension work where the governing PDEs have been passed through into the nonlinear dimensionless ODEs by using similarity transformation.

The following numerical results are noted:

- Increasing magnetic parameter decreases velocity profile, angular velocity profile and concentration profile for assisting and opposing flow whereas temperature profile is lowered.
- It has been observed that for assisting and opposing flows, the effects of the physical parameter K in the values of the velocities, temperatures, and concentration profiles are opposite of that of the magnetic field parameter.
- Higher numbers of Pr have greater influence on heat transfer since the Prandtl number rises with temperature.

- As Eckert number increases, the temperature effect also increases. Therefore, with higher values of *Ec*, their heat transfer properties are enhanced.
- Increasing Schmidt numbers lower the dimensionless concentration distributions.
- The dimensionless concentration distributions and thermophoresis parameter are increasing.
- Brownian motion parameter is increasing whereas the dimensionless concentration profiles are decreasing.
- Skin friction change with increasing values of magnetic number, Eckert number, thermophoresis parameter, Brownian motion parameter, Schmidt number, or micro-rotation, however for higher values of M, Ec, Pr, Nt, Nb, Sc and n Nusselt and Sherwood numbers are also increasing.

REFERENCES

[1] Eringen, A.C. (1964), Simple microfluids, Int. J. Eng. Sci., 2(2), 205-217.

[2] Eringen, A.C. (1965), Theory of Micropolar Continua, In: Proceedings of the Ninth Midwestern Conference, 23.

[3] Eringen, A.C. (1966) Theory of micropolar fluids, J. Math. Mech.,16(1), 1-18.

[4] Ariman, T, Turk, M.A. and Sylvester, N.D. (1973), Micro-continuum Fluid Mechanics, A Review. Int. J. Engg. Sci., 11, 905-930.

[5] Ramzan, M., Farooq, M., Hayat, T., & Chung, J. D. (2016). Radiative and Joule heating effects in the MHD flow of a micropolar fluid with partial slip and convective boundary condition. Journal of Molecular Liquids, 221, 394-400.

[6] Turk, M.A., Ariman, T and Sylvester, N.D. (1973), On Pulsatile Blood Flow, Tran. Soc. Rheol., 17, 1-21.

[7] Turk, M.A., Ariman, T and Sylvester, N.D. (1974), On Steady and Pulsatile Flow of Blood. J. Appl. Mech., 41, 1-17.

[8] Hogen, H.A. and Hensiksen, M. (1989), An Elevation of a Micropolar Model for Blood Flow Through an Idealized Stenosis, J. Biomechanics, 22, 211-218.

[9] Lee, J.D. and Eringen, A.C. (1971), Wave Propagation in Nematic Liquid Crystals, J. Chem. Phys., 54, 5027-5004.

[10] Tozeren, A. and Skalak, R. (1977), Micropolar Fluids as Models for Suspensions of Rigid Spheres, Int. J. Engg. Sci., 15, 511-523.

[11] Allen, S.J. and Kline, K.A. (1971), Lubrication Theory of Micropolar Fluids. J. Applied Mech., 38, 646-650.

[12] Chapman, T. W., & Bauer, G. L. (1975). Stagnation-point viscous flow of an incompressible fluid between porous plates with uniform blowing. Applied Scientific Research, 31(3), 223-239.

[13] Agarwal, R. S., & Dhanapal, C. (1988). Stagnation point micropolar fluid flow between porous discs with uniform blowing. International journal of engineering science, 26(3), 293-300.

[14] Takhar, H. S. and Soundalgekar, V. M. (1985), Flow and heat transfer of a Micropolar Fluid Past a Porous Plate, Indian J. Pure and Appl.,16(5), 552-558.

[15] Haq, R. U., Nadeem, S., Akbar, N. S., & Khan, Z. H. (2014). Buoyancy and radiation effect on stagnation point flow of micropolar nanofluid along a vertically convective stretching surface. IEEE transactions on nanotechnology, 14(1), 42-50.

[16] Kasiviswanathan, S. R., & Gandhi, M. V. (1992). A class of exact solutions for the magnetohydrodynamic flow of a micropolar fluid. International journal of engineering science, 30(4), 409-417.

[17] Lange, H. (1977), The existence of in stationary flows of incompressible micropolar fluids, Archive of mechanics, 29(5), 741-744.

[18] Guram, G. S., & Smith, A. C. (1980). Stagnation flows of micropolar fluids with strong and weak interactions. Computers & Mathematics with Applications, 6(2), 213- 233.

[19] Al-Sanea, S.A. (2004), Mixed convection heat transfer along a continuously moving heated vertical plate with suction or injection, Int.J. Heat Mass Transfer, 47, 1445 – 1465.

[20] Kumari, M. and Nath, G. (2004), Mixed convection boundary layer flow over thin vertical cylinder with localized injection/suction and cooling/ heating, Int. J. Heat Mass Transfer, 47, 969 –967.

[21] Wang, C. Y. (1988). Fluid flow due to a stretching cylinder. The Physics of fluids, 31(3), 466-468.

[22] Sajid, M. and Hayat, T. (2009), The application of homotopy analysis method for MHD viscous flow due to a shrinking sheet, Chaors Soliton Fractals, 39, 1317-1323.

[23] Sajid, M., Hayat, T. and Javed, T. (2008), MHD rotating flow of a viscous fluid over a shrinking surface, Non-Linear Dyn, 51(1-2), 259-265.

[24] Liao, S. (2005). A new branch of solutions of boundary-layer flows over an impermeable stretched plate. International Journal of Heat and Mass Transfer, 48(12), 2529-2539.

[25] Liao, S. (2004). On the homotopy analysis method for nonlinear problems. Applied Mathematics and Computation, 147(2), 499-513.

[26] Fang, T., & Zhang, J. (2009). Closed-form exact solutions of MHD viscous flow over a shrinking sheet. Communications in Nonlinear Science and Numerical Simulation, 14(7), 2853-2857.

[27] Ishak, A., Nazar, R. and Pop, I. (2008), Uniform suction / blowing effect on flow and heat transfer due to a stretching cylinder. Applied Mathematical Modelling, 32, 2059 – 2066.

[28] Wang. C.Y. (2008), Stagnation flow towards a shrinking sheet, International journal of Non-Linear Mechanics, 43, 377 – 382.

[29] Fang, T. and Zhang, Ji. (2009), Closed- Form exact solutions of MHD viscous flow over a shrinking sheet, Commun Nonlinear Sci Numer Sumulat, 14, 2853 –2857.

[30] Wang, C.Y. (1984), The three-dimensional flow due to a stretching flat surface, Phys. Fluids, 27(8), 1915-1917.

[31] Rahman, M.M., Uddin, M.J. Aziz, A., (2009), Effects of variable electric conductivity and non-uniform heat source (or sink) on convective micropolar fluid flow along an inclined flat plate with surface heat flux, International Journal of Thermal Sciences 48, 2331–2340.

[32] Hayat, T., Javed T., Abbas Z., (2009), MHD flow of a micropolar fluid near a stagnation-point towards a non-linear stretching surface, Nonlinear Analysis: Real World Applications, 10, 1514–1526.

[33] Anuar Ishak, Roslinda Nazar, Ioan Pop, (2008), Magnetohydrodynamic (MHD) flow of a micropolar fluid towards a stagnation point on a vertical surface, Computers and Mathematics with Applications 56, 3188-3194.

[34] Anuar Ishak, Roslinda Nazar, Ioan Pop, (2009) , MHD boundary-layer flow of a micropolar fluid past a wedge with constant wall heat flux, Communications in Nonlinear Science and Numerical Simulation 14, 109–118.

[35] Anuar Ishak, Roslinda Nazar, Ioan Pop, (2009), Dual solutions in mixed convection boundary layer flow of micropolar fluids, Communications in Nonlinear Science and Numerical Simulation 14, 1324–1333.

[36] Tarek M.A. El-Mistikawy, (2009), Limiting behavior of micropolar flow due to a linearly stretching porous sheet, European Journal of Mechanics B/Fluids 28, 253–258.

[37] Anuar Ishak, Roslinda Nazar, Ioan Pop, (2009), Dual solutions in mixed convection boundary layer flow of micropolar fluids, Communications in Nonlinear Science and Numerical Simulation 14, 1324–1333.

[38] Kumaran V., Banerjee A.K., Vanav Kumar A., Vajravelu K., (2009), MHD flow past a stretching permeable sheet, Applied Mathematics and Computation 210, 26–32.

[39] Roslinda Nazar, Norsarahaida Amin, Diana Filip, Ioan Pop, (2004), Stagnation point flow of a micropolar "fluid towards a Stretching sheet, International Journal of Non-Linear Mechanics 39, 1227 – 1235.

[40] Tasawar Hayat, Nasir Ali, Zaheer Abbas, (2007), Peristaltic flow of a micropolar fluid in a channel with different wave forms, Physics Letters A 370, 331–344.